Short-term treatment of mice with GHK peptide enhances resilience to age-related cognitive decline

Jordan Margaret Mazzola

A thesis

submitted in partial fulfillment of the

requirements for the degree of

Master of Science

University of Washington
2025

Committee:

Warren Ladiges

Brian Iritani

Christina Pettan-Brewer

Program Authorized to Offer Degree:

Comparative Medicine

University of Washington

Abstract

Short-term treatment of mice with GHK peptide enhances resilience to age-related cognitive decline

Jordan Margaret Mazzola
Chair of the Supervisory Committee:
Warren Ladiges
Department of Comparative Medicine

Age-related cognitive decline (ARCD) is a neurodegenerative process accompanied with memory loss, neuronal dysfunction, and more such as chronic inflammation and increased cellular senescence. It impacts a large percentage of the aging population, increases in prevalence with age, and is a known risk factor for more severe neurodegenerative diseases such as Alzheimer's Disease. Currently, there are no known treatments to stop or reverse the process of ARCD which presents a clear knowledge gap and opportunity to investigate potential gerotherapeutics. Glycyl-L-histidyl-L-lysine (GHK) is a naturally occurring peptide that forms complexes with copper (II) to improve wound healing and improve several age-related skin changes. Several studies have connected treatment of GHK-Cu to improvement of several hallmarks of aging via the inhibition of TGF-β and provides reasoning for exploring GHK-Cu as a potential gerotherapeutic. To test this potential, a short-term five-day treatment of GHK-Cu in middle-aged mice was performed. C57BL/6 mice, 20 to 22-months of age, were administered an intraperitoneal (IP) injection of GHK-Cu daily for five days. Cognitive function was assessed on the fifth day of treatment via a spatial navigation learning task. Several markers in the brain were assessed via immunohistochemistry (IHC) of the hippocampus and cerebellum. These markers include TGF-β1, GFAP, and phosphorylated-SMAD2 to assess the TGF-β pathway, synaptophysin and PSD95 to assess pre- and post-synaptic function, and p21 and MCP-1 to investigate cellular senescence and inflammation respectively. Aging pathways and gene regulation of GHK-Cu was investigated by RNA sequencing of the hippocampus. Results suggest improvement of cognitive function in male mice treated with GHK-Cu across several aspects including learning and memory shown via a behavioral assay, and decreased inflammation and cellular senescence. Results also revealed strong sex-dependent phenotypes within this treatment pathway as female mice treated with GHK-Cu showed less cognitive rescue when compared to male mice. This study provides support that a short-term treatment of GHK-Cu can positively impact cognitive function in middle-aged mice in a sex-dependent manner and provides potential pathways of interest for further investigation into the sex-dependent phenotypes observed. This provides support for GHK-Cu's potential as a gerotherapeutic and progress in alleviating the negative effects of ARCD.

Keywords: Aging, resilience, age-related cognitive decline (ARCD), GHK-Cu, GHK peptide, immunohistochemistry, geropathology, RNA sequencing, inflammation

Acknowledgements

I am extremely thankful to each of my committee members, Dr. Brian Iritani and Dr. Christina Pettan-Brewer, for their commitment to my success, valuable advice, and constant support. I want to give a special thanks to my mentor and committee supervisor, Dr. Warren Ladiges, for his support throughout my graduate education, offering continuous guidance, and being a strong proponent of encouraging passion for my work.

I want to offer my thanks to everyone within the Ladiges Lab. I am extremely grateful to Dr. Ruby Sue Mangalindan for her mentorship and guidance during live mouse experiments, John Morton for his logistical assistance and insuring adherence to safety protocols, Manuela Rosenfeld, Addison Keeley, and Jackson Wezeman for their constant support and help with necropsies, Kavneet Thoohan who helped with IHC, and Kathryn Spence, Dr. Soroosh Fatemie-Nainie, Katherine He, and Gerald Liao for their continuous moral support throughout this journey.

Dedication

I would like to dedicate this work to my family and friends, including but not limited to, my mom, dad, step-mom, step-dad, brother, aunt, and uncle, all of whom have supported me every step of the way. I would also like to recognize the laboratory mice who dedicate their lives to science, without them this would not be possible.

Table of Contents

Introduction

The basic biology of aging affects the functional performance of all organs in the body, including the brain. Aging often results in a decrease in resilience, defined as the ability to respond/recover from physical stressors, due to changes in pathways associated with aging (Kirkland et al., 2016). Aging of the brain can lead to other risk factors such as age-related cognitive decline (ARCD) which is a process of particular interest due to its high prevalence and public health significance (Figure 1). The prevalence of ARCD increases with increasing age, and it is predicted that approximately two-thirds of Americans will experience a level of cognitive decline by age 70 (Randhawa & Varghese, 2023, Hale et al., 2020). The global prevalence of mild cognitive impairment ranges from roughly 7% to a staggering 25% in those 60 years old and older (Eshkoor et al., 2015). ARCD can lead to a lower quality of life and loss of independence through the development of cognitive decline as brain aging progresses. There are also many cultural and clinical factors that increase risk to ARCD including lower socioeconomic status, less education, cardiovascular disease, diabetes, stroke, depression, smoking, excessive alcohol consumption, and more (Jognsiriyanyong & Limpawattana, 2018, Hugo & Ganguli, 2014, Langa & Lavine, 2014, Kivipelto et al., 2018). Additionally, people with ARCD are at an increased risk of several other neurodegenerative diseases including dementia and Alzheimer's disease (Wilson et al., 2010).

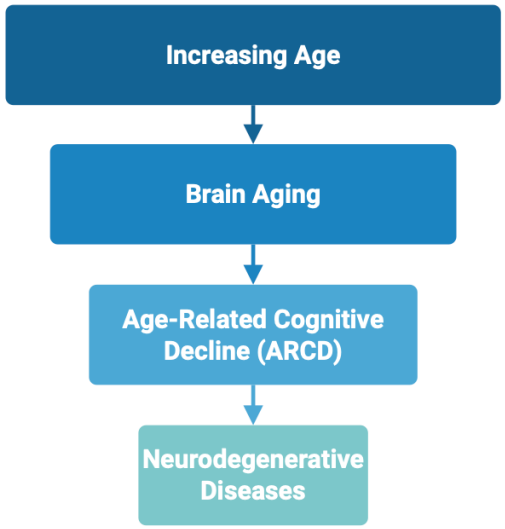

Figure 1. Flow chart displaying the progression of aging in the brain. Figure created in BioRender.com.

Recent progress in the field has led to the development of hallmarks of aging which include genomic instability, telomere attrition, loss of proteostasis, disabled macroautophagy, deregulated nutrient-sensing, mitochondrial dysfunction, cellular senescence, stem cell exhaustion, altered intercellular communication, dysbiosis, and chronic inflammation (López-Otín et al., 2023). Specifically, age-related diseases result in changes to the brain such as neuronal dysfunction, neuronal loss, and general cognitive decline in brain regions such as the hippocampus and cerebellum (Murman, 2015, Bettio et al., 2017, & Almeida et al., 2023). This neuropathology associated with ARCD in humans can result in various life altering symptoms such as decline in performance on cognitive tasks, processing information to make decisions, working memory, and cognitive function (Murman, 2015; Mayo Clinic, 2024). Despite the high prevalence and negative impacts to daily life, there are no gerotherapeutics available to reverse brain aging or ARCD which presents a serious knowledge gap and clinical shortcoming.

Glycyl-L-histidyl-L-lysine (GHK) is a naturally occurring extracellular tripeptide that readily forms complexes with copper (II) and decreases with age (Pickart et al., 1980). This peptide has been shown to be involved in wound healing through the recruitment of immune and endothelial cells, and accelerates wound healing in skin, hair follicles, boney tissue, and the gastrointestinal tract (Pickart et al., 2015). It is topically available to the general population in cosmetic formulas as it can alleviate many age-related skin changes including reducing fine lines and wrinkles, tightening loose skin, and increasing elasticity, skin density, and firmness (Pickart et al., 2015). Through utilization of the Broad Institute Connectivity Map, GHK was found to be directly involved in the mechanism of transforming growth factor-β (TGF- β) which is connected to neurodegenerative diseases and inflammation (Pickart et al., 2017). Within this mechanism, GHK was identified as a modulator of TGF-β via inhibition in bleomycin-induced pulmonary fibrosis (Zhou et al., 2017). TGF-β is a regulatory cytokine identified to be a key modulator of reactive astrocytes and is thus a target of interest in astrocyte regulation (Luo, 2022). The proposed mechanism features extracellular activation of TGF-β and the SMAD-dependent signaling pathway (Luo, 2022). The ability for GHK-Cu to cross the blood-brain-barrier and exhibit antioxidant effects in brain tissue provides compelling reasoning for exploring GHK-Cu as a neurotherapeutic for brain aging, ARCD, and other neurodegenerative diseases that are associated with an increase in reactive oxygen species (Pickart et al., 2017).

Preliminary observations with the naturally occurring peptide GHK have suggested that it has an effect in deterring ARCD by delaying brain aging. Several *in vitro* studies have been performed to observe the effect of GHK on cellular senescence and other aging pathways. GHK treatment of C57BL/6 (B6) primary lung fibroblast cells reduced p21 and p53 expression which are both markers of cellular senescence and can promote fibrosis (He et al., 2024, Hecker et al., 2014). Through this study, it was also found that the primary lung fibroblasts treated with GHK exhibited enhanced contraction compared to control fibroblasts which provides evidence of GHK's capability to resolve collagen scarring (He et al., 2025). An *in vitro* study observing the effect of GHK-Cu on LPS-induced cellular senescence in a mouse N2A neuronal cell line also saw a decrease senescence of the treated cells compared to the controls through a senescent-specific β-galactosidase assay (unpublished data, Ladiges Lab). Similar results were observed *in vivo* B6 mouse models with several parameters revealing robust results in response to a treatment of GHK-Cu. A dose of 15 mg/kg was shown to be effective while staying well below both the lethal dose (LD50) of GHK-Cu in mice which is 320 mg/kg, in addition to a copper toxicity level of 35 mg/kg (Pickart & Margolina, 2018, Liu et al., 2020).

In a three-week study, intraperitoneal (IP) injections of GHK-Cu at a dose of 15 mg/kg were administered five times a week to 28-month-old B6 mice. When testing their cognitive function in a spatial navigation learning task after the injections, male mice treated with GHK-Cu found the escape hole faster than male mice receiving saline as the control (unpublished data, Ladiges Lab). An eight-week study saw robust results in both male and female 23-month-old B6 mice treated with a 15 mg/kg dose of GHK-Cu administered intranasally. These male and female mice treated with GHK-Cu for eight weeks displayed improved cognitive function in both a spatial navigation learning task and the Y-maze behavioral assay by locating the escape hole faster and experiencing increased percent alternation respectively when compared to control cohorts receiving saline (unpublished data, Ladiges Lab). In a five-day experiment exploring the relationship between a five-day IP treatment of a 15 mg/kg dose of GHK-Cu and sleep deprivation in 20-month-old B6 mice, an improvement in cognitive function was observed in the spatial navigation learning task in male mice treated with GHK-Cu that did not undergo sleep deprivation (unpublished data, Ladiges Lab). These observations suggest that a short-term five-

day IP treatment of GHK-Cu in middle-aged B6 mice is an appropriate model for brain aging and developing ARCD.

Additionally, the C57BL/6 mouse model provides a translationally relevant model for ARCD. Mouse models are generally advantageous due to their short lifespan and ability for more control over experimental conditions compared to human clinical trials or experiments with other mammals. A study revealed that cognitive impairment in C57BL/6 mice was present, and the severity depended on the age of the mice (Daneshjoo et al., 2022). It was shown that 28-month-old C57BL/6 mice experienced the worst cognitive impairment in the radial tread maze compared to other groups (Daneshjoo et al., 2022). The 20-month-old mice in this study performed slightly better but revealed more cognitive deficits than the 12-month and 4-month-old mice (Daneshjoo et al., 2022). This provides reasoning for utilizing the 20-month-old C57BL/6 mouse model as they are experimentally advantageous and exhibit signs of an ARCD mouse model in relation to humans of similar cognitive impairment (Figure 2).

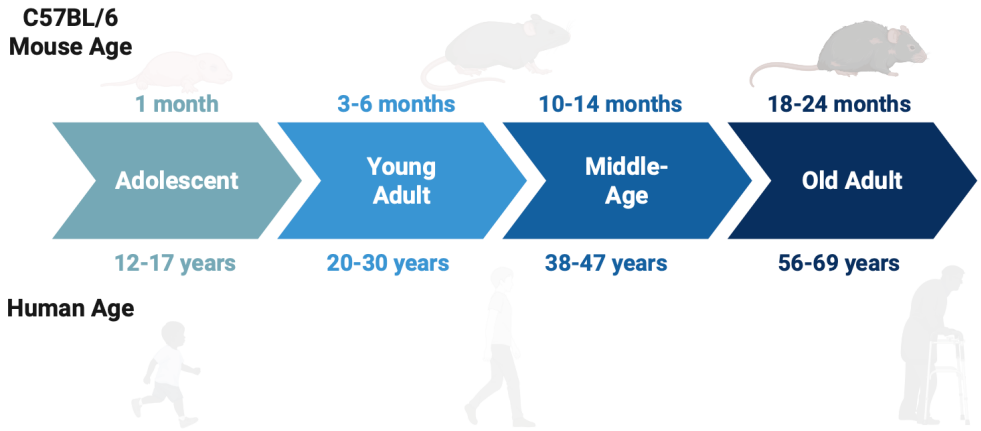

Figure 2. Timeline detailing C57BL/6 mouse model age (in months) in relation to human age (in years) from McWain et al., 2022). Figure created in BioRender.com.

Astrocytes are essential non-neuronal glial cells that perform several important functions within the central nervous system (CNS). Their diverse functions include synapse formation and function management, maintaining neurotransmitter release and uptake, production of trophic factors, and more (Matias et al., 201). Astrocytes contain neuroprotective phenotypes with anti-inflammatory factors and activation of neuroprotective cytokines but can contain reactive toxic phenotypes when activated. These reactive phenotypes have been shown to result in exacerbated injuries of the spinal cord, increased β-amyloid production, and a loss of neuroprotective functions which can contribute to developing or worsening ARCD (Matias et al., 2019). Additionally, this reactive toxic phenotype is known to increase with age, specifically within the hippocampus and frontal cortex regions of the brain (Nichols et al., 1993). A specific negative phenotype termed “astrosenescence” is observed with senescent astrocytes overexpressing classic cellular senescent markers of p16, p21, and p53 (Cohen & Torres, 2019). This astrosenescent accumulation is tied to increases in reactive oxygen species (ROS), inflammation, and mitochondrial dysfunction which are all significant factors in identified pathways of aging and contribute to ARCD (Cohen & Torres, 2019 & López-Otín et al., 2023).

This study proposes that a short-term treatment of GHK-Cu for five days enhances resilience of ARCD by targeting astrocytes and TGF-β in middle-aged mice. Aim 1 of this study was designed to characterize behavioral phenotypic features of middle-aged C57BL/6 of both sexes

treated with a short-term five-day administration of GHK-Cu peptide. Aim 2 of this study was designed to investigate molecular pathways of TGF-β via immunohistochemistry, as well as discover large numbers of genes in the brain affected by GHK-Cu via RNA sequencing in brains of middle-aged mice of both sexes treated with GHK-Cu peptide.

Materials & Methods

Mice. This study used 30 male and 30 female 20-21-month-old C57BL/6J mice from the National Institute of Aging Aged Rodent Colony. The mice were housed in a 14:10 light cycle pathogen-free facility with diet and water provided ad libitum. Procedures were approved through UW IACUC protocol and safe handling practices were followed. All mice received an ear punch for identification after a two-week acclimation period following delivery. They were weighed weekly and had cage changes every other week. Male and female mice were randomly divided in half with 15 mice receiving the treatment and 15 mice receiving the control for each sex. The treatment and control were administered once a day for five consecutive days at a consistent time across all five days. On the fifth day, the mice underwent an assay and were sacrificed by carbon dioxide (CO_2) asphyxiation. Brains and main body organs were immediately harvested, sectioned, and either flash frozen in liquid nitrogen (LN_2) and stored in -80°C or immersed in 10% neutral buffered formalin (NBF). Tissues immersed in 10% NBF were allowed to fix for 72 hours, transferred to 70% ethanol, and were embedded in paraffin wax by the Ladiges Lab Histology Core. Brains were sectioned into 4 µm sagittal slices for immunohistochemistry. Figure 3 displays the experimental timeline described above with a five-day treatment of GHK-Cu via intraperitoneal (IP) injections.

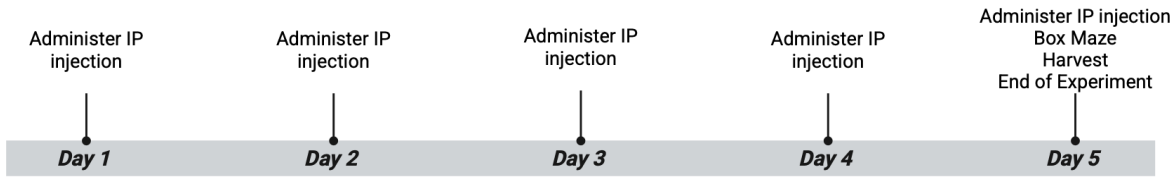

Figure 3. Experimental timeline adhered to by all cohorts. Figure created in BioRender.com.

Treatment. The treated cohort received an intraperitoneal (IP) injection of the copper complex of glycyl-L-histidyl-L-lysine (Creative Peptides: CPC1613) once a day for five consecutive days between 8 AM and 10 AM. The dosage was determined to be 15 mg/kg which is well under the potential copper toxicity dose of 35 mg/kg of body weight with each dose only containing 2.1 mg/kg of copper (Tucker et al., 2023; Liu et al., 2020). Weights of the mice within the cohort from the previous week were averaged and used to calculate the amount of GHK-Cu needed in each dose. The GHK-Cu treatment was prepared within 72 hours prior to the first treatment administration and took place within a BSL-1 safety hood. The GHK-Cu solution was aliquoted, filtered through sterile syringe filters (Avantor: 76479-024), and diluted with a sterile saline solution (sodium chloride 0.9%) to reach 200 µL per dose. IP injections were performed with sterile 28G 0.5 mL insulin syringes (BD Insulin Syringes: 329461). The injection site alternated sides every day and was thoroughly cleaned prior to injections with sterile alcohol prep pads. Mice in the control cohort received an IP injection of 200 µL of the sterile saline solution following the same parameters.

Box Maze. Box Maze is a spatial navigation learning task used to determine the degree of cognitive impairment as an endpoint assay after treatment (Darvas et al., 2020). The maze is comprised of a large clear plastic box lined with reflective material and a bright light positioned above to provide a mild stressor. There are seven false exits closed off with a PVC cap and a

true exit comprised of three short PVC pipes that lead to a dark rest cage. Each side of the box contains a large image as well as a smaller image above each exit hole. One mouse is evaluated at a time with the assessment beginning by placing the mouse in the center of the box. It is given 120 seconds to solve the maze by entering the true exit into the rest cage. If the mouse is not successful within 120 seconds, it is guided to the true exit. The mouse is allowed to rest for 30 seconds in the rest cage, then is returned to the home cage for 90 seconds. This assessment is repeated three additional times to produce four total trials. In between trials, the maze and rest cage are sprayed with 70% ethanol and wiped down. In between cages, the maze, rest cage, PVC caps, and PVC pipes are thoroughly sprayed with 70% ethanol and dried before beginning the next cage of mice. Figure 4 provides a visual representation of the Box Maze assay featuring the box, eight holes with seven of them leading to PVC caps and being attached to PVC piping leading to a rest cage.

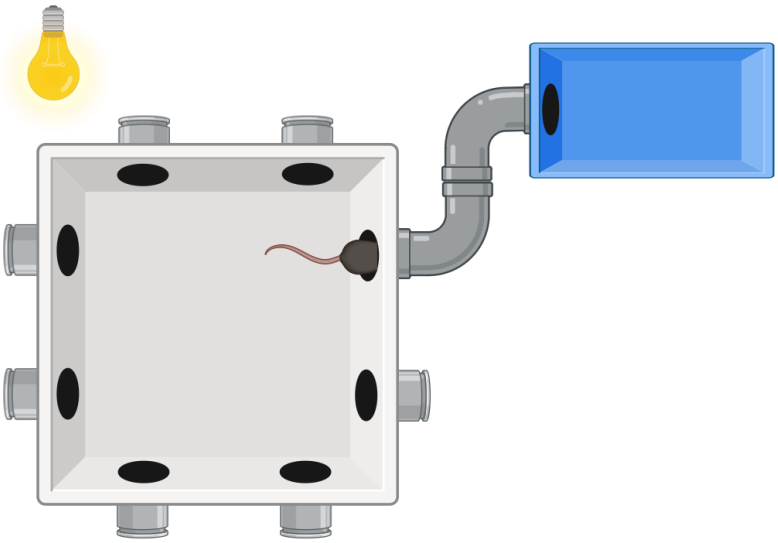

Figure 4. Box maze layout featuring a mouse exiting through the exit hole into the rest cage. Figure created in BioRender.com.

Immunohistochemistry. Brains from all 60 mice were cut into 4 µm sagittal slices on charged slides for immunohistochemistry (IHC). Staining was completed with an Abcam kit (HRP/DAB Rabbit kit: 64621). Slides underwent hydration by being placed in xylene, 100% ethanol, 95% ethanol, 70% ethanol, and deionized (DI) water. Antigen retrieval followed the hydration process with slides being submerged in either citric acid buffer or Tris-EDTA and placed in a water bath set to 98°C. Slides were removed from the water bath and reached room temperature, a hydrophobic barrier was applied around the tissue, slides were dipped in TBST, then incubated with a hydrogen peroxidase block for 10 minutes. After, slides were washed in TBST three times for five minutes each, incubated with a protein block for 10 minutes, washed in TBST three times for five minutes each, and incubated overnight with the primary antibody diluted with TBST at 4°C. The next day, slides were washed in TBST three times for five minutes each, incubated with biotinylated goat anti-rabbit for 10 minutes, washed in TBST three times, incubated with streptavidin peroxidase for 10 minutes, washed in TBST three times, incubated in DAB chromogen diluted with DAB substrate, washed in TBST twice, washed in DI water once for five minutes, then dehydrated by being placed in 70% ethanol, 95% ethanol, 100% ethanol, and xylene. After the dehydration process, hydrophobic mounting media was placed on the slides and slide covers were applied. The following primary antibodies were used with the above procedure: 1/250 Synaptophysin (Invitrogen: MA5-16402), 1/250 PSD95 (Abcam: ab18258),

1/50 phospho-SMAD2 (Invitrogen: 44-244G), 1/800 MCP-1 (Novus: NBP1-07035), and 1/200 p21 (Abcam: ab188224). A multi-chromogen stain protocol was also utilized with an Abcam kit (HRP/DAB Rabbit kit: 64621) and Novodiax kit (IHC Magenta 1:1 kit: K50011-030). The multi-chromogen follows the DAB chromogen protocol outlined above closely; however, slides were washed in TBST for three minutes and incubated in 300 mM sulfuric acid following DAB incubation as opposed to the wash and dehydration steps. Following the sulfuric acid incubation, slides were washed in TBST three times, incubated in hydrogen peroxidase block for 10 minutes, and adhered to the protocol above for the remainder of staining with an overnight incubation of the second antibody. In place of the DAB chromogen and substrate, the slides were incubated in a 1:1 dilution of magenta chromogen and substrate for the second antibody. The primary antibody stained using the DAB chromogen was 1/50 TGF-ß1 (Abcam: ab215715) and the secondary antibody staining using the magenta chromogen was 1/1500 GFAP (Invitrogen: PA1-10019).

Image Processing. Slides that underwent IHC were photographed at 20x and 40x magnification using the NIS-D microscope (Nikon Instruments Inc.). Images were analyzed with QuPath (version 0.4.3) which assessed the percent area stained as well as the optical density which quantifies the intensity of the DAB and magenta stain in that region. The hippocampus and cerebellum were the regions of interest for neuropathological evaluation.

RNA Sequencing. A total of 12 samples, three from each cohort, of flash frozen sections of hippocampus were randomly selected to undergo RNA extraction, purification, and sequencing. Tissues were removed from -80°C, weighed, and RNA was extracted by placing the samples in 2 mL tubes with ceramic beads (ThermoFisher: 15-340-153) and homogenized in Trizol via a Bead Mill. RNA was crudely separated from non-RNA material by centrifuging the homogenized mixture and transferring the supernatant. RNA purification included phase separation Rand RNA precipitation. Phase separation was comprised of incubation, adding chloroform, centrifuging the samples, and separating the aqueous phase. RNA precipitation several cycles of washing and centrifuging in isopropanol and 75% ethanol. Once the pellet of RNA was present and dried, 50 µL of Nuclease-Free Water (Qiagen: 1039480) and spun down to result in the RNA sample. The NanoDrop spectrophotometer was used to measure the concentration (ng/µL), A260/A280, and A260/A230 ratios. A column-based cleanup was used to further clean the RNA using the RNeasy Mini Kit (Qiagen: 74104). Several cycles of washing and centrifuging with the RLT buffer, ethanol, RW1 buffer, and RPE buffer. The sample was eluted with 30 µL of Nuclease-Free Water and evaluated with the NanoDrop a second time. The samples were stored in -80°C and delivered to Novogene for sequencing with a shotgun approach. Novogene completed a quality control analysis prior to sequencing, and every sample passed with a RNA Integrity Number (RIN) of 7.3 and above. After isolation, samples were processed by Novogene (Novogene.com) using the Illumina Novoseq X-Plus platform resulting in bulk-mRNA paired-end fastq files. For analysis, the browser-based cluster computing platform SciDAP (SciDAP.com) was used. The SciDAP analysis pipeline is available online at https://github.com/datirium. Experimental samples were aligned using Trim-Galore and Star with the mm10 mouse genome as the reference genome. Differential expression between sample cohorts was generated using DESeq2, where the false discovery rate was set to 0.1 and adjusted using the Wald test. GSEA analysis was generated using the Hallmark gene sets (GSEA) and significance for the false discovery rate was set at 0.1. All RNA quantification was performed within the SciDAP pipeline. All RNA statistics were performed within the SciDAP pipeline. All DESeq2 and GSEA data visuals were generated within the SciDAP pipeline.

Statistics. For comparing the means between two groups and assessing for significant differences, two-sample t-test was used. For assessing significant differences between more

than two cohorts, one-way ANOVA was used. For multiple comparisons between multiple cohorts, two-way ANOVA was used with the Geisser-Greenhouse correction. Spearman's correlation was utilized for correlation analysis between two data sets to yield a p-value and Spearman's rank correlation coefficient (r). Analysis of the RNA sequencing library was performed through a bioinformatics platform SciDAP (see section above for more details). The spatial navigation task will be analyzed using a statistical model termed the "Learning Index" and is a weighted system aimed at normalizing the dataset to more accurately reflect population-wide cognition (Park et al., 2024). Variance was calculated for each trial and provided variance ratios for each trial in relation to Trial 1. For each mouse the performance time was taken for Trials 2-4, divided by the performance time of Trial 1, subtracted by 1, then multiplied by the respective trial variance ratio. The output values for Trials 2-4 were added together to form the learning index where mice with higher values displayed more optimal learning capability and cognition compared to those with lower values. All statistical analyses, graphs, and p-values were generated in GraphPad Prism (version 10.2.3) and significance was determined at $p < 0.05$.

Results

Male mice treated with GHK-Cu experience improved cognition compared to mice treated with saline.

Both male and female mice participated in a spatial navigation learning task, the box maze, on the last day of the experiment following five days of treatment or control administration. The box maze helps to assess their capacity for learning and memory by recording how fast a mouse can escape through the escape hole, and if they can retain that information throughout the four trials. The Learning Index Score factors in population variance and a higher score is indicative of greater cognitive function. The male mice treated with GHK-Cu for five days have a significantly higher Learning Index Score than the control male mice who received the saline (Figure 5A). This data suggests an increase in cognitive function, learning capability, and memory retention in male mice who received the treatment. There was no significant difference observed in the female mice who were treated with GHK-Cu for five days compared to those who received the control (Figure 5B). This suggests that the phenotypes associated with the treatment of GHK-Cu are sex-dependent with males, but not females, showing improved cognition.

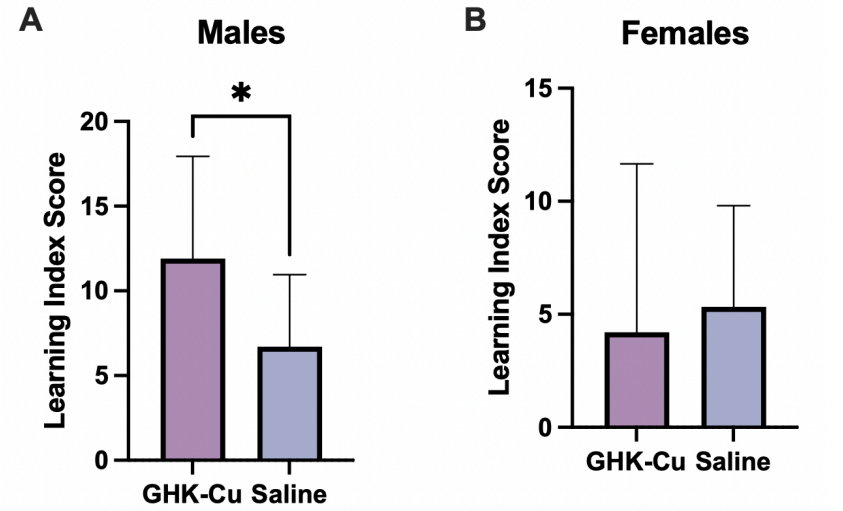

Figure 5. Learning index scores of male and female mice who received an IP injection of GHK-Cu (treatment) or Saline (control) for five days. A. Learning index scores of 20-month-old C57BL/6 male mice treated with GHK-Cu (treatment) or saline (control). B. Learning index scores of 20-month-old C57BL/6 female mice treated with GHK-Cu (treatment) or saline (control). T-test: $p<0.05$, n=10-12/cohort.

Male mice treated with GHK-Cu experience faster escape times in spatial navigation learning task compared to control cohort.

Another assessment of cognitive function in the spatial navigation learning task is the time it takes the mouse to enter the escape hole, from the time the trial begins to when the mouse has its head and all four paws in the escape hole. This parameter, known as escape time, can be anywhere from 0-120 seconds with a quicker escape time correlating to increased cognitive function, learning ability, and memory. An additional indication of increased cognitive function is a decrease in escape time as the trials progress. Male mice that received the five-day GHK-Cu treatment exhibit a significant difference in escape time compared to male mice who received the control for both Trials 1 and 2 (Figure 6A). Additionally, the GHK-Cu treated males had a significantly lower escape time in Trials 2 and 3 when compared to Trial 1 (Figure 6A). This trend was not observed in the saline males which suggests an increased cognitive function in GHK-Cu treated males versus the males that received saline. This data reveals sex differences again, with the difference in cognitive function does not present in females given GHK-Cu when compared to those who received saline (Figure 6B). Aside from a difference in escape time from Trial 1 to 2 in saline females, there were no other statistically significant differences (Figure 6B). This means that unlike males treated with GHK-Cu, the females treated with GHK-Cu did not experience faster escape times or improved cognition.

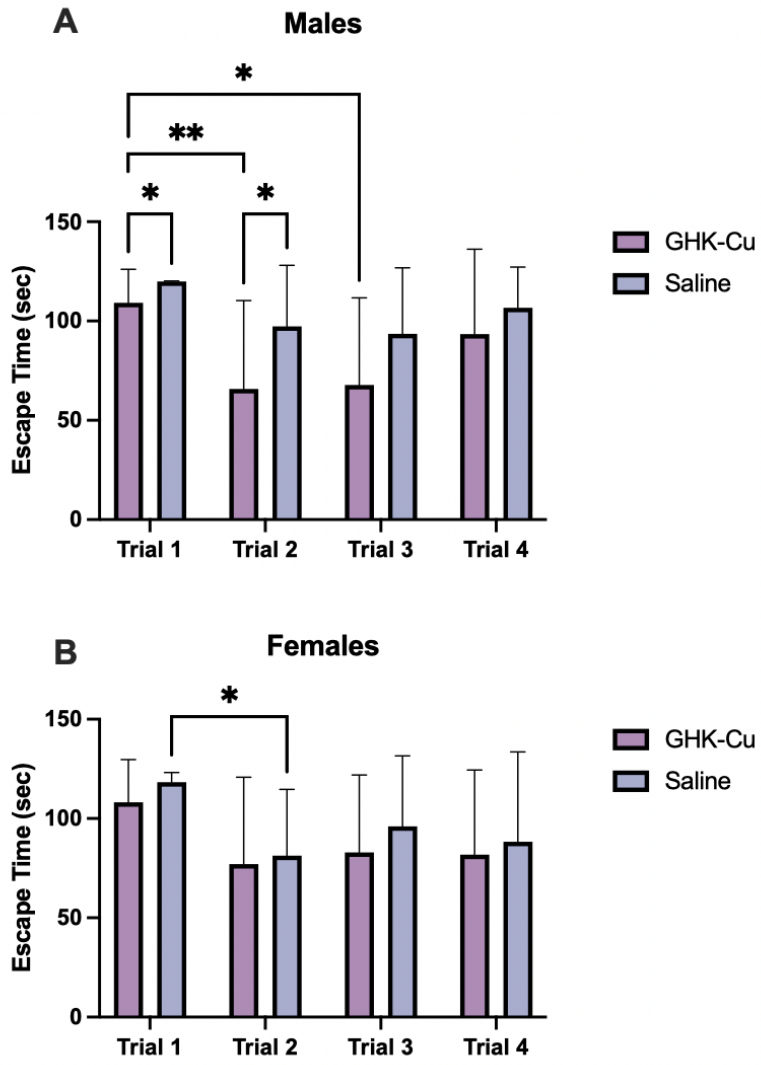

Figure 6. Box maze escape times for treated and control cohorts of both sexes across all four trials. A. The time it took in seconds for 20-month-old C57BL/6 male mice to enter the escape hole. B. The time it took in seconds for 20-month-old C57BL/6 female mice to enter the escape hole. Two-way ANOVA: $p<0.05$, n=10-12/cohort.

Male mice treated with GHK-Cu show increased exploratory behavior compared to mice treated with saline.

Several parameters were measured while the mice were in the box maze for each trial, including the number of times they reared. A majority of these rears were “supported rearing” where their rear was supported by the wall of the maze or the PVC used to secure the PVC caps and piping. In an open field test, supported rearing was discussed as an exploratory behavior as opposed to increased anxiety (Sturman et al., 2018). For each trial, the number of rears was divided by the time the mouse was in the box maze to normalize the time variable. When observing the number of rears per second within each trial, both males and females treated with GHK-Cu had increased values when compared with the control cohorts (Figure 7A & 7B). In males, this increase is observed in trial 2 whereas in females it is observed in trials 1 and 2 (Figure 7A & 7B). When observing the average number of rears per second across all four trials within each cohort, there is a notable significant difference between the females

treated with GHK-Cu and females that received the saline control (Figure 7C). Again, the females treated with GHK-Cu experience increased rearing per second, indicating an increase in exploratory behavior compared to the females who received saline. Rearing per second in males treated with GHK-Cu was significantly higher than the female control group but was not when compared to the male control group which highlights additional phenotypic sex differences. (Figure 7C). This means that females receiving saline showed the lowest indication of exploratory behavior, and both males and females treated with GHK-Cu showed significantly higher levels of exploratory behavior when compared to that cohort.

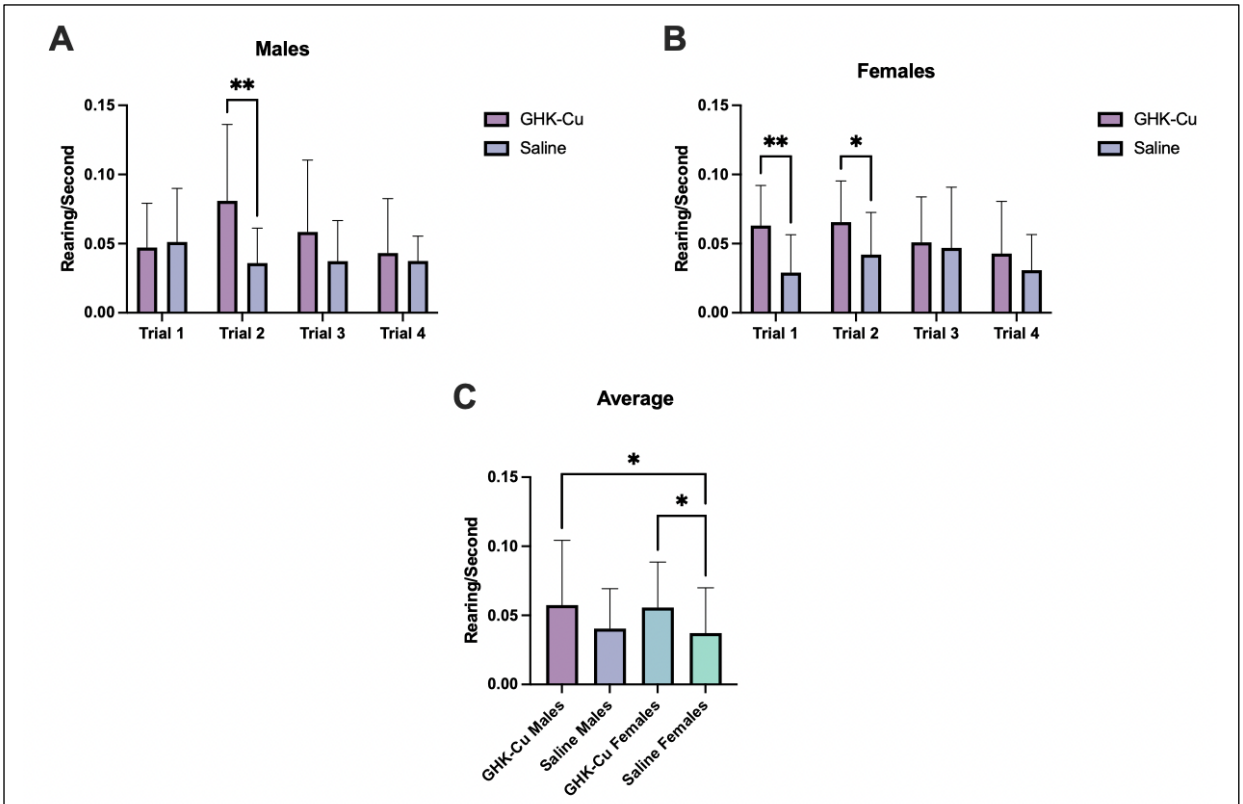

Figure 7. Number of rears per second in box maze of both sexes across all four trials and averaged by cohort. A. The number of rears per second of 20-month-old C57BL/6 male mice for each box maze trial. B. The number of rears per second of 20-month-old C57BL/6 female mice for each box maze trial. C. The number of rears per second averaged over all trials per cohort for both sexes. Two-way ANOVA (A & B) and One-way ANOVA (C): $p<0.05$, n=15/cohort.

Number of false exits entered reveals sex difference between males treated with GHK-Cu and females treated with GHK-Cu.

An additional parameter assessed during the spatial navigation learning task was the number of false exits each mouse entered during a trial prior to escaping through the escape hole. An increased number of escape attempts through one of the seven false exits contained in the maze can indicate decreased cognitive function due to a lack of memory retention and learning of where the false exits are located. When broken down by sex and trial, there were no significant differences in the number of false exits entered aside from a decrease in the males that received saline in trial 2 when compared to trial 4 (Figure 8A & 78B). The number of false exits entered was also assessed by taking the average across all trials within each cohort. This revealed the males treated with GHK-Cu had a significant lower number of false exit attempts when compared to females receiving GHK-Cu (Figure 8C). This indicates that with a five-day treatment of GHK-Cu, male mice have significantly lower parameter that is associated with improved cognitive impairment when compared to female mice under the same experimental

conditions. This, along with the additional box maze data presented, reveals substantial sex differences amongst the treated cohorts.

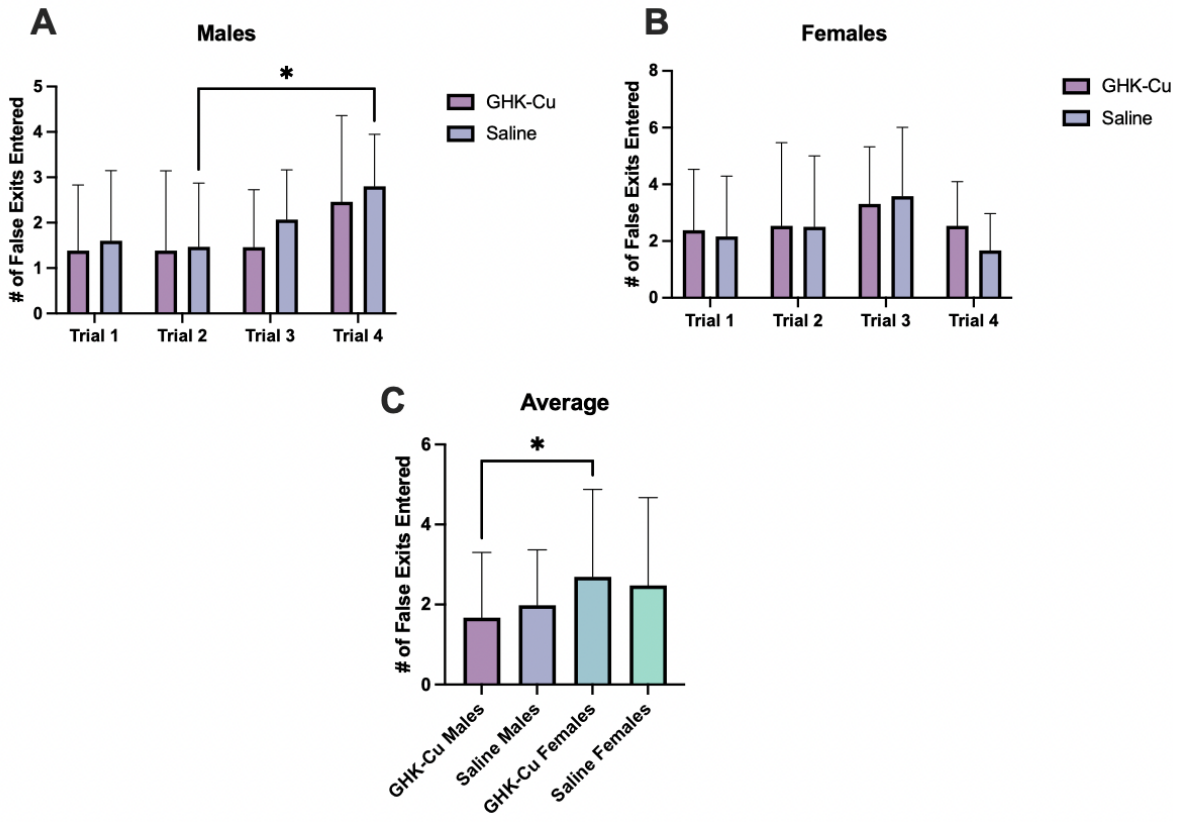

Figure 8. Number of false exits entered in box maze of both sexes across all four trials and averaged by cohort. A. The number of false exits entered of 20-month-old C57BL/6 male mice for each box maze trial. B. The number of false exits entered of 20-month-old C57BL/6 female mice for each box maze trial. C. The number of false exits entered averaged over all trials per cohort for both sexes. Two-way ANOVA (A & B) and One-way ANOVA: $p<0.05$, n=10-12/cohort.

TGF-β1 is decreased in male mice treated with GHK-Cu in both the hippocampus and cerebellum.

TGF-β1 is a well-known target of GHK-Cu and is heavily involved in the SMAD2/SMAD3 pathway as an astrocyte regulator. IHC was performed to assess TGF-β1 in the hippocampus and cerebellum. Male mice treated with GHK-Cu displayed a decreased positive stain percentage of TGF-β1 expression compared to males receiving saline in both the hippocampus and cerebellum, however females treated with GHK-Cu did not display this phenotype in either region (Figure 9A & 9D). When assessing TGF-β1 staining intensity via mean optical density, it was revealed that females treated with GHK-Cu had a greater staining intensity versus the female control cohort in both brain regions (Figure 9B & 9E). Male mice treated with GHK-Cu had a non-significant trend of decreased staining intensity when compared to the control cohort, differing from the female results (Figure 9B & 9E). Factoring the positive stain area and mean optical density together, male mice treated with GHK-Cu once again displayed decreased levels in hippocampal and cerebellar regions compared to males receiving saline, however no significant difference was observed in the females (Figure 9C & 9F). These results affirm the involvement of TGF-β1 in the expected GHK-Cu treatment effects in males in multiple regions

and may provide an area of interest when exploring sex-dependent differences across the behavioral and molecular assays.

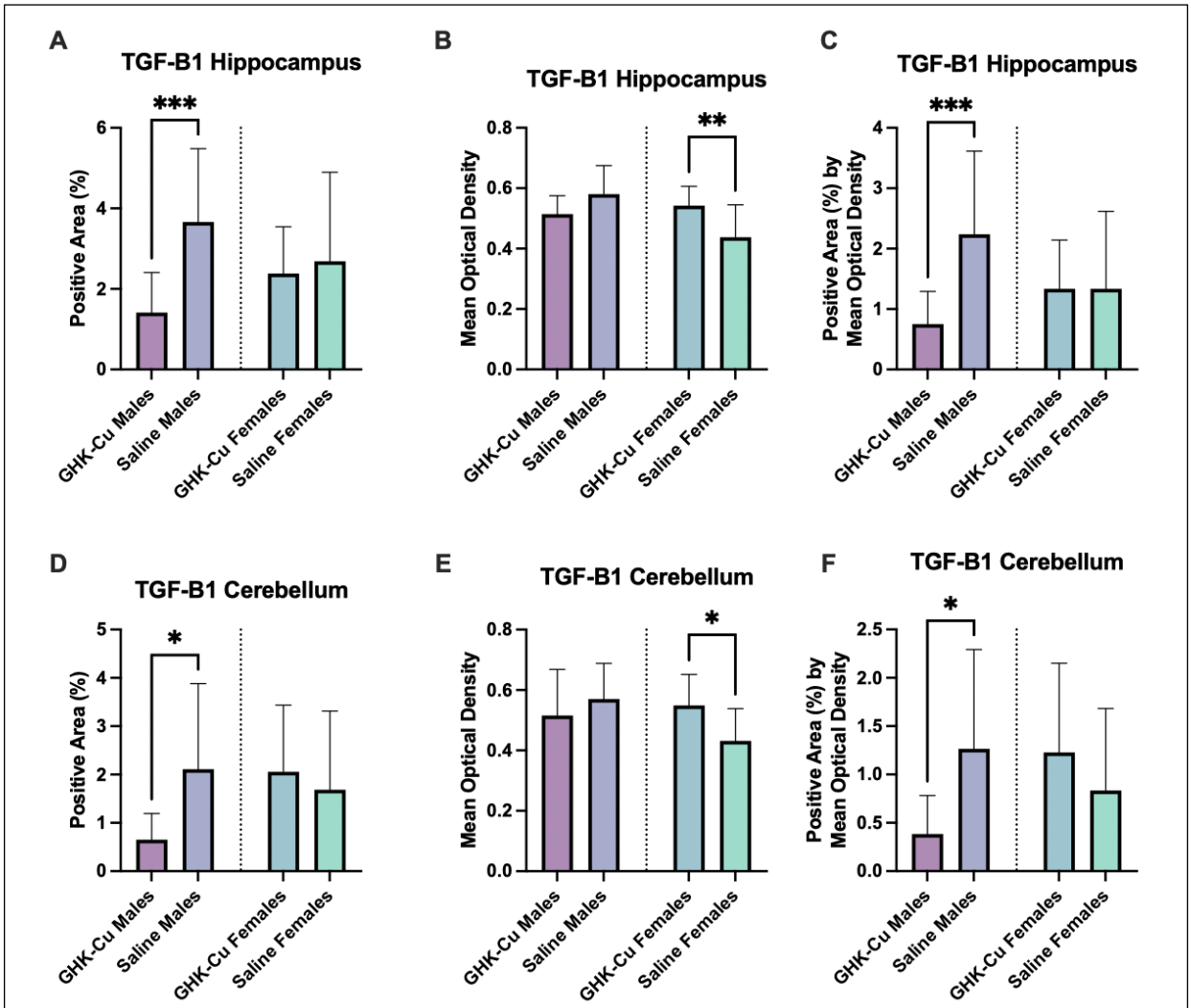

Figure 9. Immunohistochemistry staining of TGF-β1 expression in the hippocampal and cerebellar brain regions of C57BL/6 20-month-old mice of both sexes treated with GHK-Cu or saline. A. Percentage of the area stained positive for TGF-β1 expression in the hippocampus. B. Mean optical density of TGF-β1 expression in the hippocampus. C. Percentage of the area stained positive for TGF-β1 expression multiplied by the mean optical density in the hippocampus. D. Percentage of the area stained positive for TGF-β1 expression in the cerebellum. E. Mean optical density of TGF-β1 expression in the cerebellum. F. Percentage of the area stained positive for TGF-β1 expression multiplied by the mean optical density in the cerebellum. One-way ANOVA: $p<0.05$, n=15/cohort.

Male mice treated with GHK-Cu show decreased levels of astrocytes in both the hippocampus and cerebellum compared to the control cohort.

Reactive astrocyte phenotypes can have detrimental effects to an aging brain and are regulated through the TGF-β1 pathway. To further investigate this pathway and molecular relationship with GHK-Cu, IHC staining of GFAP, an astrocytic marker, was performed on the hippocampal and cerebellar regions. Expression of GFAP, denoted by the percentage of area stained, revealed a significant decrease of GFAP expression in males treated with GHK-Cu in both brain regions (Figure 10A & 10D). Females treated with GHK-Cu did not reveal this phenotype, but there is a non-significant trend of decreased GFAP expression in the cerebellum (Figure 10A &

10D). Staining intensity of GFAP was decreased in males treated with GHK-Cu compared to the control cohort, however this was only observed in the hippocampus (Figure 10B & 10E). Females treated with GHK-Cu revealed an increased staining intensity in both the hippocampus and cerebellum versus the control cohort (Figure 10B & 10E). When expression via positive area stained and staining intensity were evaluated together, males treated with GHK-Cu displayed a significant decrease in levels of GFAP compared to males receiving saline in both brain regions (Figure 10C & 10F). These results largely mirror trends in TGF-β1 expression provide additional information in investigating why sex-dependent phenotypes are present.

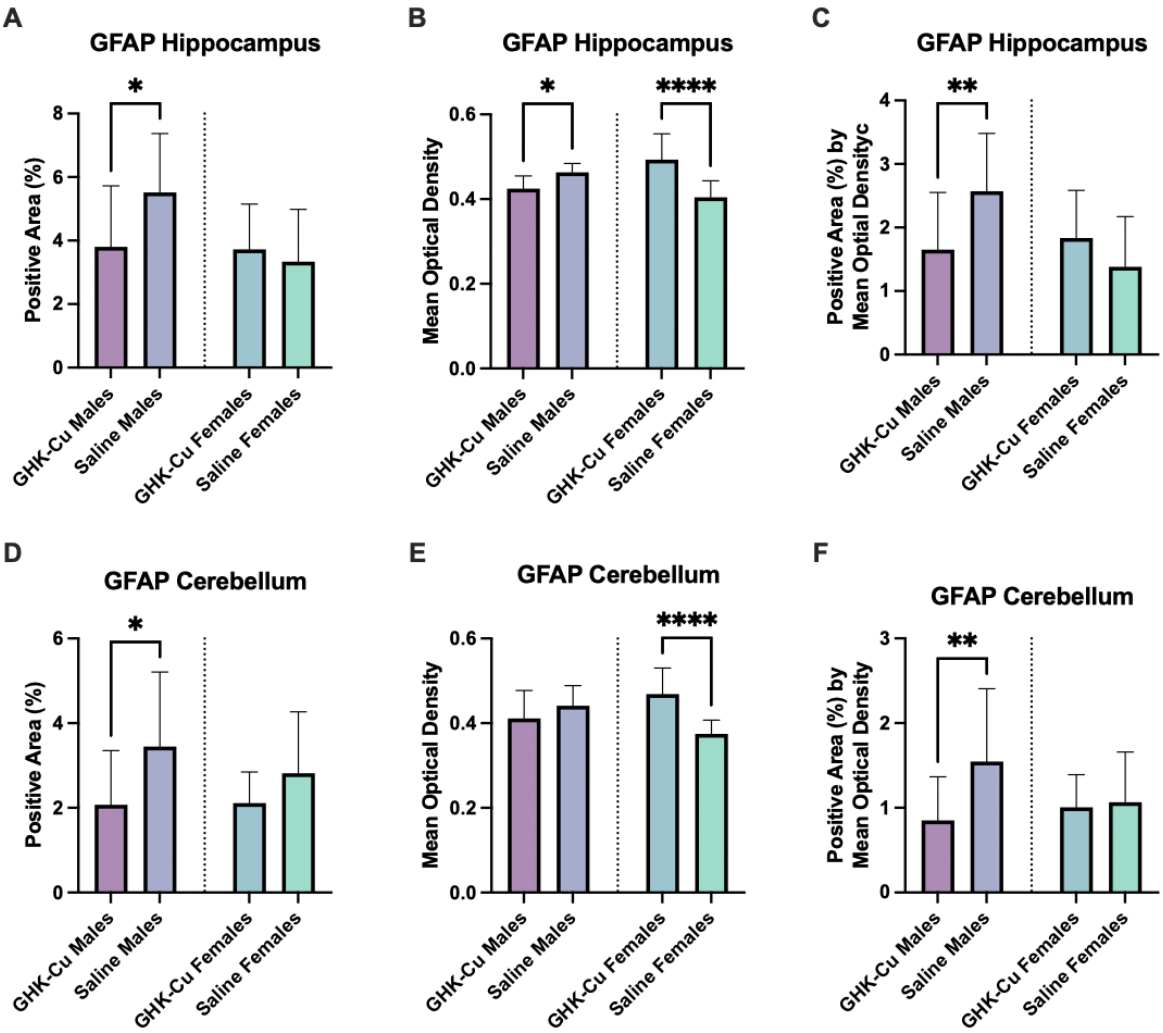

Figure 10. Immunohistochemistry staining of GFAP expression in the hippocampal and cerebellar brain regions of C57BL/6 20-month-old mice of both sexes treated with GHK-Cu or saline. A. Percentage of the area stained positive for GFAP expression in the hippocampus. B. Mean optical density of GFAP expression in the hippocampus. C. Percentage of the area stained positive for GFAP expression multiplied by the mean optical density in the hippocampus. D. Percentage of the area stained positive for GFAP expression in the cerebellum. E. Mean optical density of GFAP expression in the cerebellum. F. Percentage of the area stained positive for GFAP expression multiplied by the mean optical density in the cerebellum. One-way ANOVA: $p<0.05$, n=15/cohort.

TGF-β1 and GFAP expression is correlated in the hippocampus, but not the cerebellum.

TGF-β1 and GFAP staining was performed as a double stain on the same slides and are hypothesized to be closely linked in the TGF-β pathway. A correlation analysis was performed to assess the correlation and linear relationship between TGF-β1 positive stain percentage and GFAP positive stain percentage. Figure 11A displays the correlation of the stain in the hippocampus amongst all the cohorts, not stratified for sex or treatment. Figure 11A reveals a significant correlation between the TGF-β1 and GFAP positive stain percentages in the hippocampus. When these values were stratified by sex and treatment group, the staining in the hippocampus of GHK-Cu treated male mice did not maintain this significant correlation, but the GHK-Cu treatment female mice did (Figure 11B & 11C). In exploring this correlation and relationship between the TGF-β1 and GFAP positive stain percentages in the cerebellum, there was no observed statistically significant correlation overall or sex and treatment stratified (Figure 11D-F). Potential reasons for the difference could be a higher variability within the hippocampus of the GHK-Cu treated male mice and the cerebellum region as a whole. This indicates a stronger correlation between these two antibodies in the hippocampus when compared to the cerebellum.

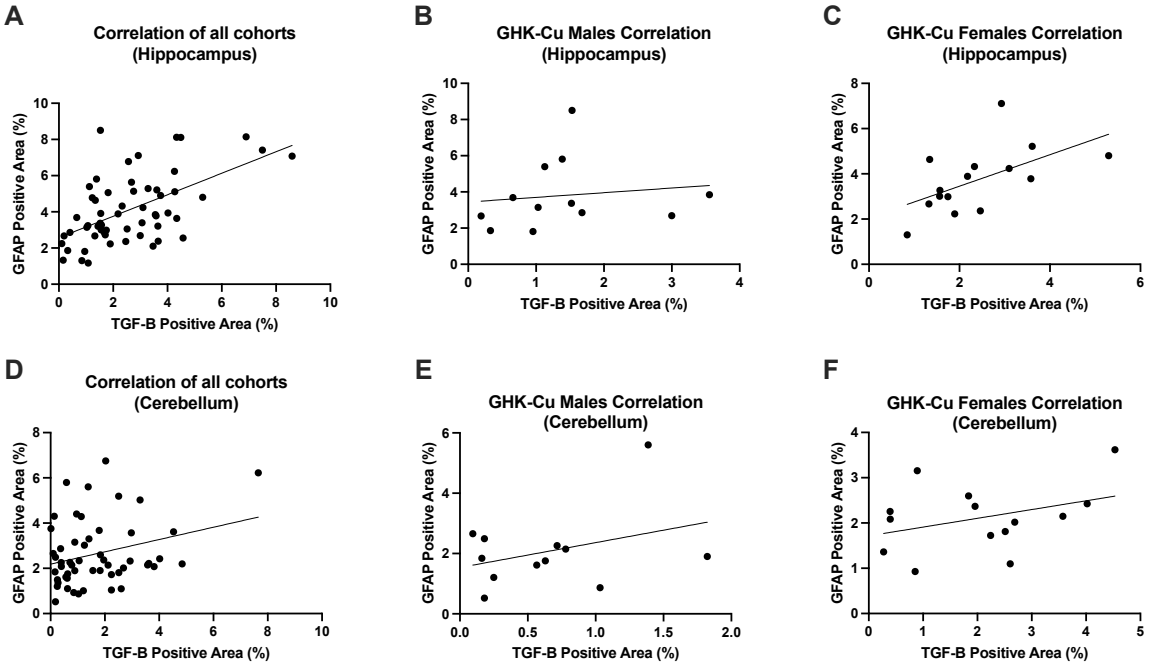

Figure 11. Correlation analysis of the TGF-β1 and GFAP double stain positive staining percentages in the hippocampal and cerebellar regions of C57BL/6 20-month-old mice of both sexes treated with GHK-Cu or saline. A. Correlation analysis of the TGF-β1 and GFAP positive staining percentages in the hippocampus of all mice across all cohorts r=0.5081 & p<0.0001. B. Correlation analysis of the TGF-β1 and GFAP positive staining percentages in the hippocampus of GHK-Cu treated male mice r=0.4266 & p=0.1689. C. Correlation analysis of the TGF-β1 and GFAP positive staining percentages in the hippocampus of GHK-Cu treated female mice r=0.6036 & p<0.05. D. Correlation analysis of the TGF-β1 and GFAP positive staining percentages in the cerebellum of all mice across all cohorts r=0.1887 & p=0.1760. E. Correlation analysis of the TGF-β1 and GFAP positive staining percentages in the cerebellum of GHK-Cu treated male mice r=0.0909 & p=0.7830. F. Correlation analysis of the TGF-β1 and GFAP positive staining percentages in the cerebellum of GHK-Cu treated female mice r=0.2791 & p=0.3332. Spearman's correlation: p<0.05, n=15/cohort.

Phosphorylated-SMAD2 expression is similar across treatment cohorts, sexes, and brain regions.

As it is theorized that SMAD2/3 are involved in astrocyte regulation via the TGF-β1 pathway when phosphorylated, IHC staining of phosphorylated-SMAD2 was performed in the hippocampal and cerebellar regions across cohorts. There was no significant difference observed in either sex or brain region when evaluating percent area of positive staining or when positive staining area was factored in with mean optical density (Figure 11A, 11C, 11D, & 11F). Despite this, both males and females display a non-significant trend of decreased phosphorylated-SMAD2 levels for positive area stained in both brain regions and positive area factored with mean optical density in the hippocampus (Figure 11A, 11C, & 11D). In exploring staining intensity, mean optical density, as a stand-alone, females treated with GHK-Cu display a higher intensity compared to the control cohort in the hippocampus, but not cerebellum (Figure 11B & 11E). This offers valuable information for further investigation as to what mechanisms are involved in astrocyte regulation within the TGF-β1 pathway.

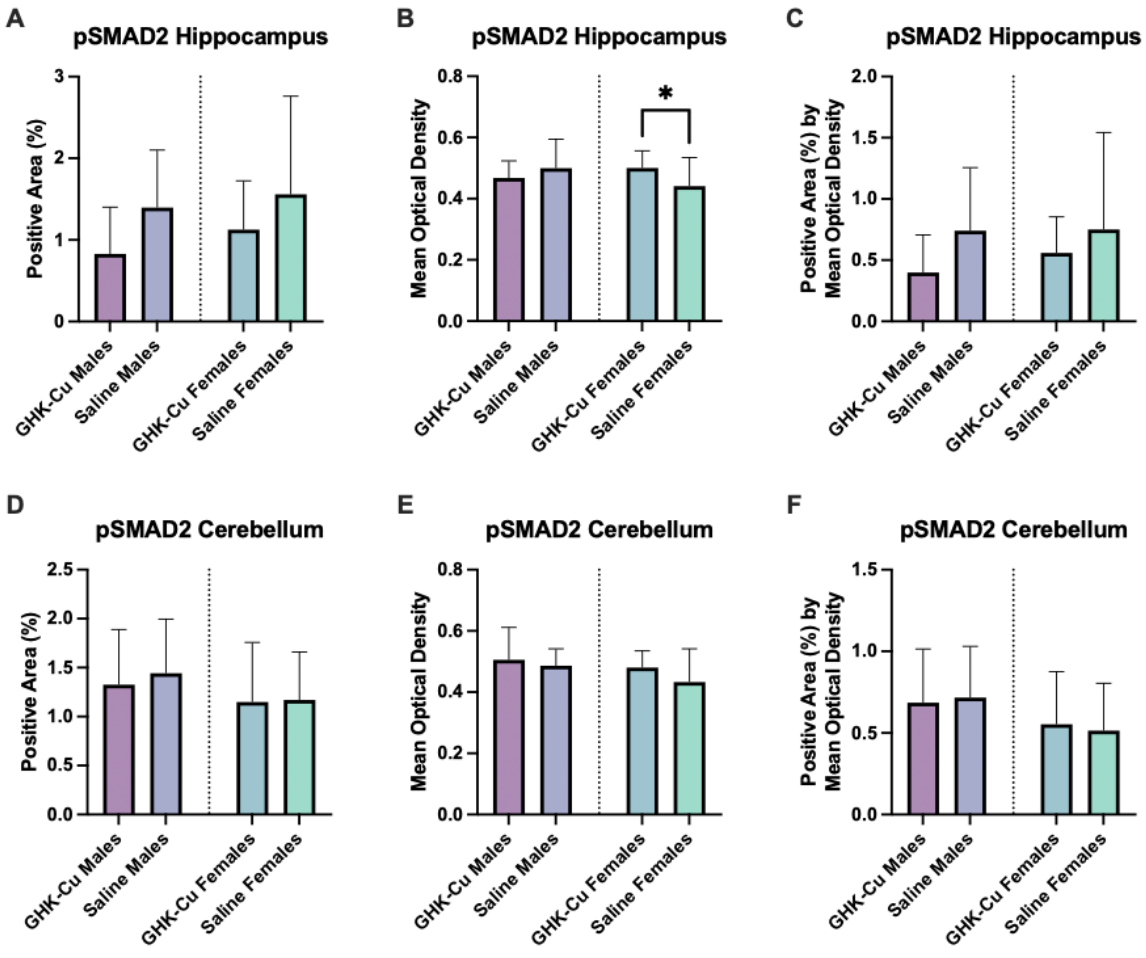

Figure 12. Immunohistochemistry staining of phospho-SMAD2 expression in the hippocampal and cerebellar brain regions of C57BL/6 20-month-old mice of both sexes treated with GHK-Cu or saline. A. Percentage of the area stained positive for phospho-SMAD2 expression in the hippocampus. B. Mean optical density of phospho-SMAD2 expression in the hippocampus. C. Percentage of the area stained positive for phospho-SMAD2 expression multiplied by the mean optical density in the hippocampus. D. Percentage of the area stained positive for phospho-SMAD2 expression in the cerebellum. E. Mean optical density of phospho-SMAD2 expression in the cerebellum. F. Percentage of the area stained positive for phospho-SMAD2 expression multiplied by the mean optical density in the cerebellum. One-way ANOVA: $p<0.05$, n=15/cohort.

Synaptophysin levels remain stable across all cohorts and sexes after GHK-Cu treatment with similar trends observed in hippocampal and cerebellar tissue.

Synaptophysin, a biomarker of pre-synaptic health and function, is heavily influenced by astrocytes as a method for neuronal maintenance and synaptic formation. Synaptophysin was evaluated via IHC of the hippocampus and cerebellum regions of C57BL/6 mice. The percent area of positive synaptophysin staining in both the hippocampus and cerebellum did not reveal any significant differences between treated and control cohorts of both male and female mice treated with GHK-Cu for 5 days (Figure 12A & 12D). The mean optical density, displaying the staining intensity of Synaptophysin, also remained stable across the treated and control cohort within each sex, with that similar pattern remaining conserved across the two brain tissue regions (Figure 12B & 12E). In assessing the percent area of positive stain and staining intensity together, the same trend remained consistent with so significant differences between treated and control cohorts of both sexes (Figure 12C & 12F). This may indicate that a longer treatment of GHK-Cu is needed to impact pre-synaptic health and maintenance.

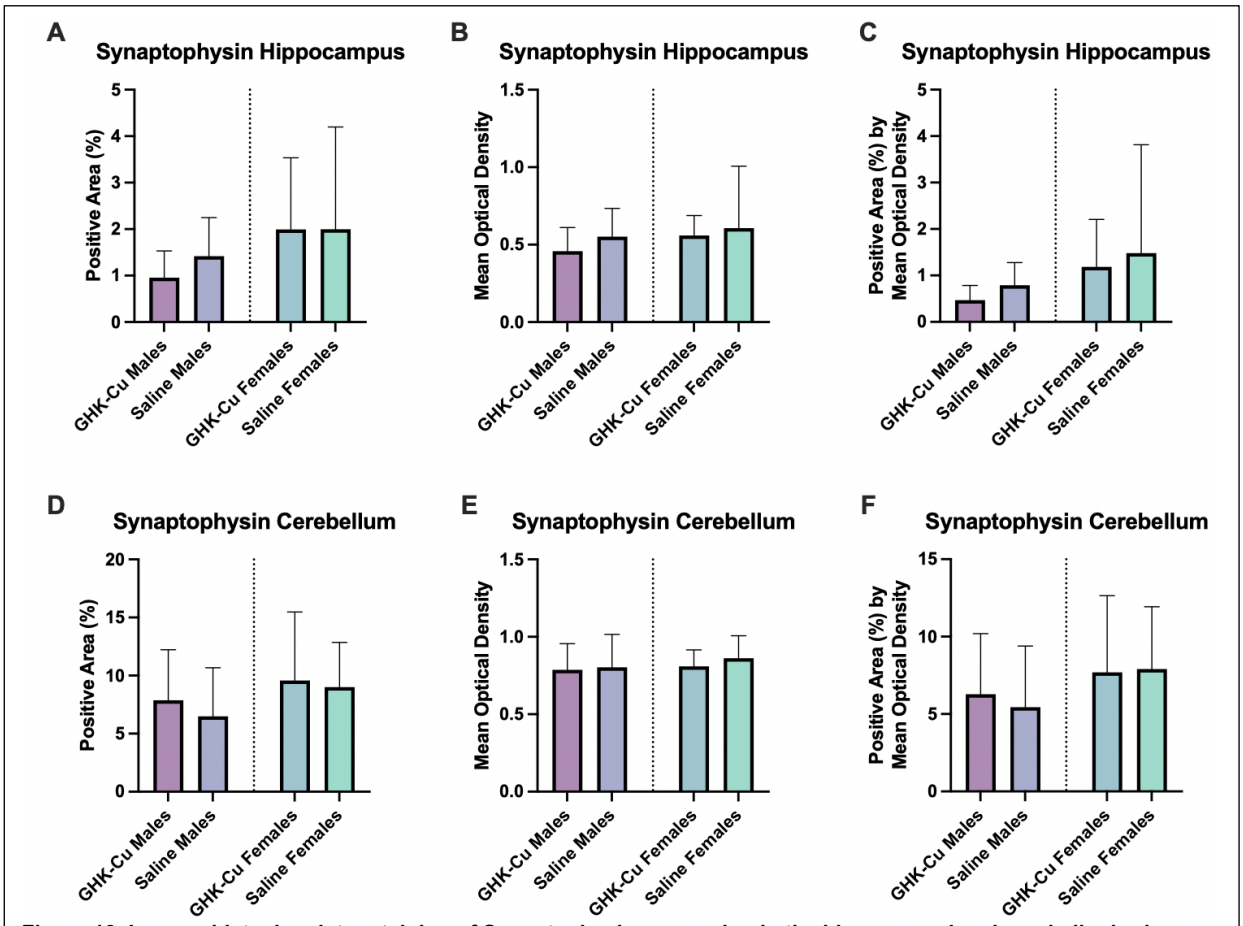

Figure 13. Immunohistochemistry staining of Synaptophysin expression in the hippocampal and cerebellar brain regions of C57BL/6 20-month-old mice of both sexes treated with GHK-Cu or saline. A. Percentage of the area stained positive for Synaptophysin expression in the hippocampus. B. Mean optical density of Synaptophysin expression in the hippocampus. C. Percentage of the area stained positive for Synaptophysin expression multiplied by the mean optical density in the hippocampus. D. Percentage of the area stained positive for Synaptophysin expression in the cerebellum. E. Mean optical density of Synaptophysin expression in the cerebellum. F. Percentage of the area stained positive for Synaptophysin expression multiplied by the mean optical density in the cerebellum. One-way ANOVA: $p<0.05$, n=15/cohort.

PSD95 levels remain stable across all cohorts and sexes after GHK-Cu treatment with similar trends observed in hippocampal and cerebellar tissue.

PSD95 is a marker utilized to assess post-synaptic function and health which, much like Synaptophysin, is heavily related to astrocyte regulation in relation to neuronal maintenance. IHC of the hippocampus and cerebellum of C57BL/6 mice treated with GHK-Cu for 5 days revealed similar trends across cohorts and sexes. The percent area of positive stain among the treatment versus control group did not reveal any significant differences among males and females in the hippocampus, though there was a non-significant trend of higher PSD95 levels in males treated with GHK-Cu compared to the control group in the cerebellum (Figure 13A & 13D). This trend is displayed in the graphs depicting the percent area of positive stain and staining intensity together with no significance between treated versus non-treated cohorts, however there is a non-significant increase in PSD95 in males treated with GHK-Cu when compared to the control group in the cerebellum (Figure 13C & 13F). The staining intensity, displayed via mean optical density, also did not reveal any significant differences between the treated and control cohorts of either sex of both brain regions (Figure 13B & 13E). The trends of no significance observed in PSD95 are extremely similar to those observed with Synaptophysin staining and indicate consistencies in neuronal maintenance in relation to GHK-Cu.

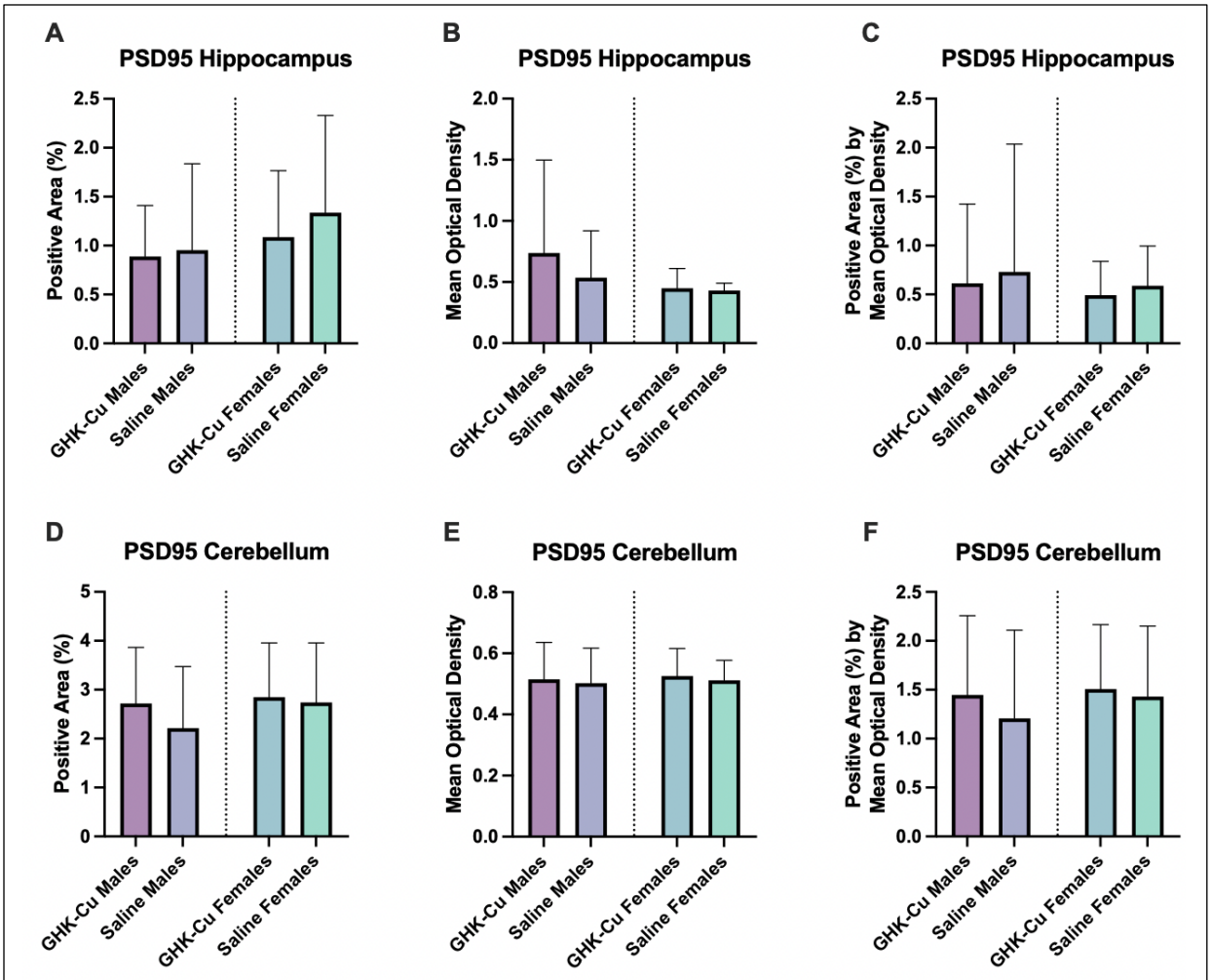

Figure 14. Immunohistochemistry staining of PDS95 expression in the hippocampal and cerebellar brain regions of C57BL/6 20-month-old mice of both sexes treated with GHK-Cu or saline. A. Percentage of the area stained positive for PSD95 expression in the hippocampus. B. Mean optical density of PSD95 expression in the hippocampus. C. Percentage of the area stained positive for PSD95 expression multiplied by the mean optical density in the hippocampus. D. Percentage of the area stained positive for PSD95 expression in the cerebellum. E. Mean optical density of PSD95 expression in the cerebellum. F. Percentage of the area stained positive for PSD95 expression multiplied by the mean optical density in the cerebellum. One-way ANOVA: $p<0.05$, n=15/cohort.

Decreased senescence was observed in brains from mice treated with GHK-Cu in a sex and region-dependent manner.

In order to assess molecular pathways in several regions of the brain, immunohistochemistry (IHC) staining was utilized. p21 is a marker of cellular senescence which is a hallmark of aging and increases with developing ARCD. The percentage of positive area denotes the percentage of pixels containing a positive stain when compared to the number of total pixels of the image. In the hippocampus, female mice treated with GHK-Cu had a significant decrease in positive area of p21 expression compared to female mice who received the saline control (Figure 14A). This phenotype was maintained in the cerebellum, in addition to males treated with GHK-Cu also seeing a decrease in p21 expression when compared to males receiving the control (Figure 14C). Mean optical density is utilized to assess the intensity level of staining across images. In the hippocampus, no differences were observed between p21 staining intensity in GHK-Cu treated and control cohorts of either sex, but the cerebellum revealed a decrease in p21 staining

intensity in males treated with GHK-Cu compared to the males receiving saline (Figure 14B & 14E). When assessing the percent area stained and staining intensity together, females treated with GHK-Cu had decreased values in both the hippocampus and cerebellum when compared to the control cohort, and males treated with GHK-Cu had decreased p21 values in the cerebellum, but not the hippocampus versus males who received saline (Figure 14C & 14F). This indicates GHK-Cu decreasing levels of cellular senescence in a sex-dependent manner that is also influenced by brain region but may not be based on the TGF-β1 pathway due to the lack of differences observed in the TGF-β1 and GFAP staining of female mice seen in Figure 9 & Figure 10.

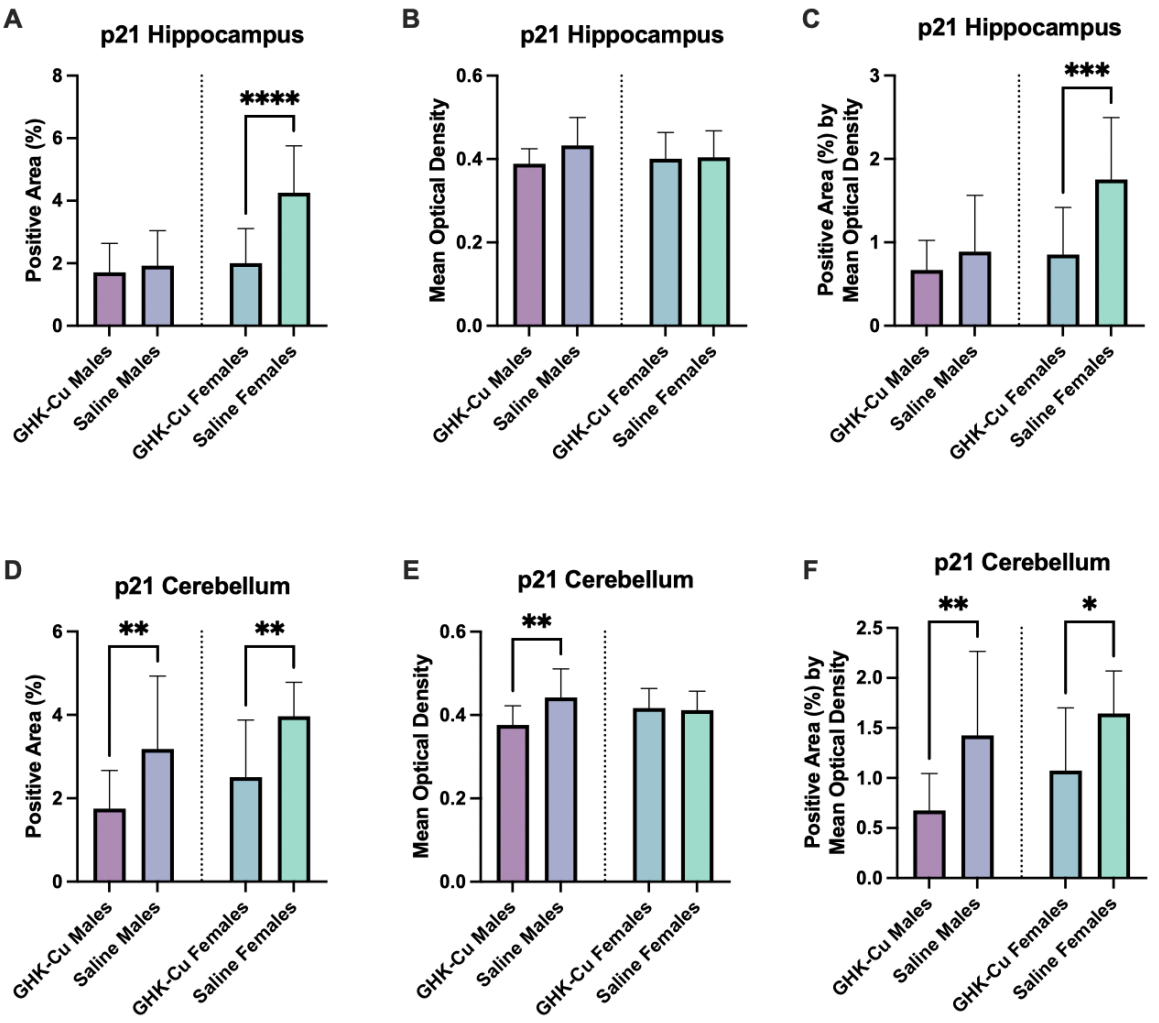

Figure 15. Immunohistochemistry staining of p21 expression in the hippocampal and cerebellar brain regions of C57BL/6 20-month-old mice of both sexes treated with GHK-Cu or saline. A. Percentage of the area stained positive for p21 expression in the hippocampus. B. Mean optical density of p21 expression in the hippocampus. C. Percentage of the area stained positive for p21 expression multiplied by the mean optical density in the hippocampus. D. Percentage of the area stained positive for p21 expression in the cerebellum. E. Mean optical density of p21 expression in the cerebellum. F. Percentage of the area stained positive for p21 expression multiplied by the mean optical density in the cerebellum. One-way ANOVA: $p<0.05$, n=15/cohort.

Male mice treated with GHK-Cu showed decreased neuroinflammation in both the hippocampus and cerebellum compared to the control cohort.

MCP-1 is a chemoattractant of inflammatory molecules and was used as a marker of neuroinflammation via IHC staining of the hippocampus and cerebellum. The percent area of positive MCP-1 staining in both hippocampus and cerebellum was decreased in males treated with GHK-Cu versus males who received the control, but females treated with GHK-Cu only displayed a non-significant trend in the cerebellum when compared to the female control cohort (Figure 15A & 15D). Staining intensity of MCP-1 assessed via mean optical density revealed a significant decrease in GHK-Cu treated males versus saline males, but was region-specific to the hippocampus (Figure 15B & 15E). MCP-1 staining intensity in females treated with GHK-Cu followed the same trend as positive staining percentage with a non-significant trending decrease observed in the cerebellum when comparing the GHK-Cu treated cohort to the saline cohort (Figure 15B & 15E). In assessing the product of positive area stained and mean optical density of MCP-1, the phenotype displayed with positive percent area stained in Figure 14A and 14D was conserved in both males and females treated with GHK-Cu across both brain regions (Figure 15C & 15F). These findings reveal that a treatment of GHK-Cu is associated with a decrease of neuroinflammation in male mice in a sex-dependent manner and is conserved in both the hippocampal and cerebellar brain regions.

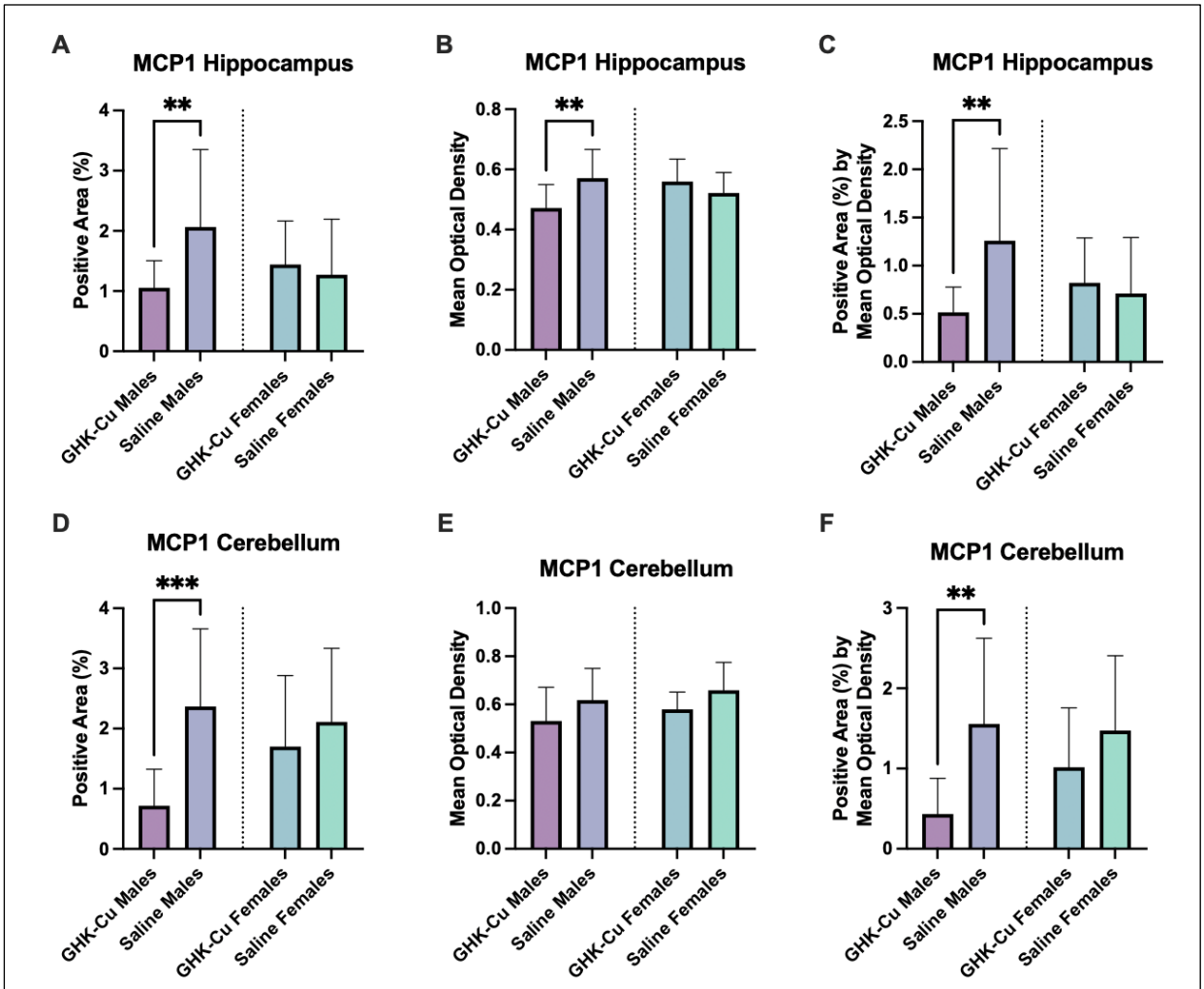

Figure 16. Immunohistochemistry staining of MCP-1 expression in the hippocampal and cerebellar brain regions of C57BL/6 20-month-old mice of both sexes treated with GHK-Cu or saline. A. Percentage of the area stained positive for MCP-1 expression in the hippocampus. B. Mean optical density of MCP-1 expression in the hippocampus. C. Percentage of the area stained positive for MCP-1 expression multiplied by the mean optical density in the hippocampus. D. Percentage of the area stained positive for MCP-1 expression in the cerebellum. E. Mean optical density of MCP-1 expression in the cerebellum. F. Percentage of the area stained positive for MCP-1 expression multiplied by the mean optical density in the cerebellum. One-way ANOVA: $p<0.05$, n=15/cohort.

RNA-sequencing reveals various brain aging pathways in female mice are improved with a five-day treatment of GHK-Cu.

RNA isolation and sequencing was completed on hippocampal tissue of GHK-Cu treated and control cohorts of both sexes. Differential gene expression and gene set enrichment analysis (GSEA) were completed to explore differences in gene expression and within the hallmark gene sets between the treated and control cohorts. Each enrichment plot displays the normalized enrichment score (NES) which assesses the significance and direction of gene expression, the p-value, and the false discovery rate (FDR). The enrichment score (ES) on the y-axis represents if the genes within the pathways of interest are upregulated, above the zero threshold, or downregulated, below the zero threshold. The “UV_Response_DN” pathway represents genes that are downregulated when cells are exposed to ultraviolet (UV) radiation whereas the “UV_Response_UP” pathway represents genes that are upregulated with exposed to UV radiation. Figure 15A and 15B displays a significant downregulation and upregulation

respectively when comparing female mice treated with GHK-Cu to the control cohort receiving saline. Another pathway related to DNA damage and response is DNA repair which is up regulated in female mice treated with GHK-Cu versus saline (Figure 16C). Upregulation of the DNA repair pathway has a NES of 5.575 which indicates strong clustering of genes within that pathway and reflects the higher ES value (Figure 16C). Oxygenation and energy production throughout the body is imperative and the hippocampal tissue of female mice treated with GHK-Cu revealed an up regulation of genes involved in the oxidative phosphorylation pathway (Figure 16D), however there was also an upregulation observed with reactive oxygen species (ROS) and hypoxia pathways (Figure 16E & 16F). The upregulation of genes associated with the oxidative phosphorylation pathway have a higher NES value of 4.965 when compared to the NES values of the ROS and hypoxia pathways which indicates increased clustering and gene upregulation (Figure 16D, 16E, & 16F). E2F and p53 are both transcription factors involved in regulating the cell cycle and regulate cellular senescence, and both are upregulated in female treated mice compared to female mice who received the control (Figure 16G & 16H). The mitotic spindle assists in segregating chromosomes during cell division and the genes associated with this pathway are downregulated in treated female mice (Figure 16I). TNF-α signaling via NF-κB is a pathway with several functions including regulating inflammation and apoptosis. This pathway was upregulated in the female treated cohort compared to the control cohort (Figure 16J). “MYC_Targets_V1” refers to a broad subset of genes relating to myelocytotic oncogene (MYC) which is a transcription factor that regulates cell growth, proliferation, and differentiation. This pathway was found to be upregulated in female treated mice, following the trend of E2F and p53 that are also transcription factors involved in cell cycle regulation (Figure 16K, 16G, & 16H). Lastly, protein secretion which is involved in cell-to-cell communication and homeostasis was downregulated in female mice treated with GHK-Cu compared to the saline cohort (Figure 16L).

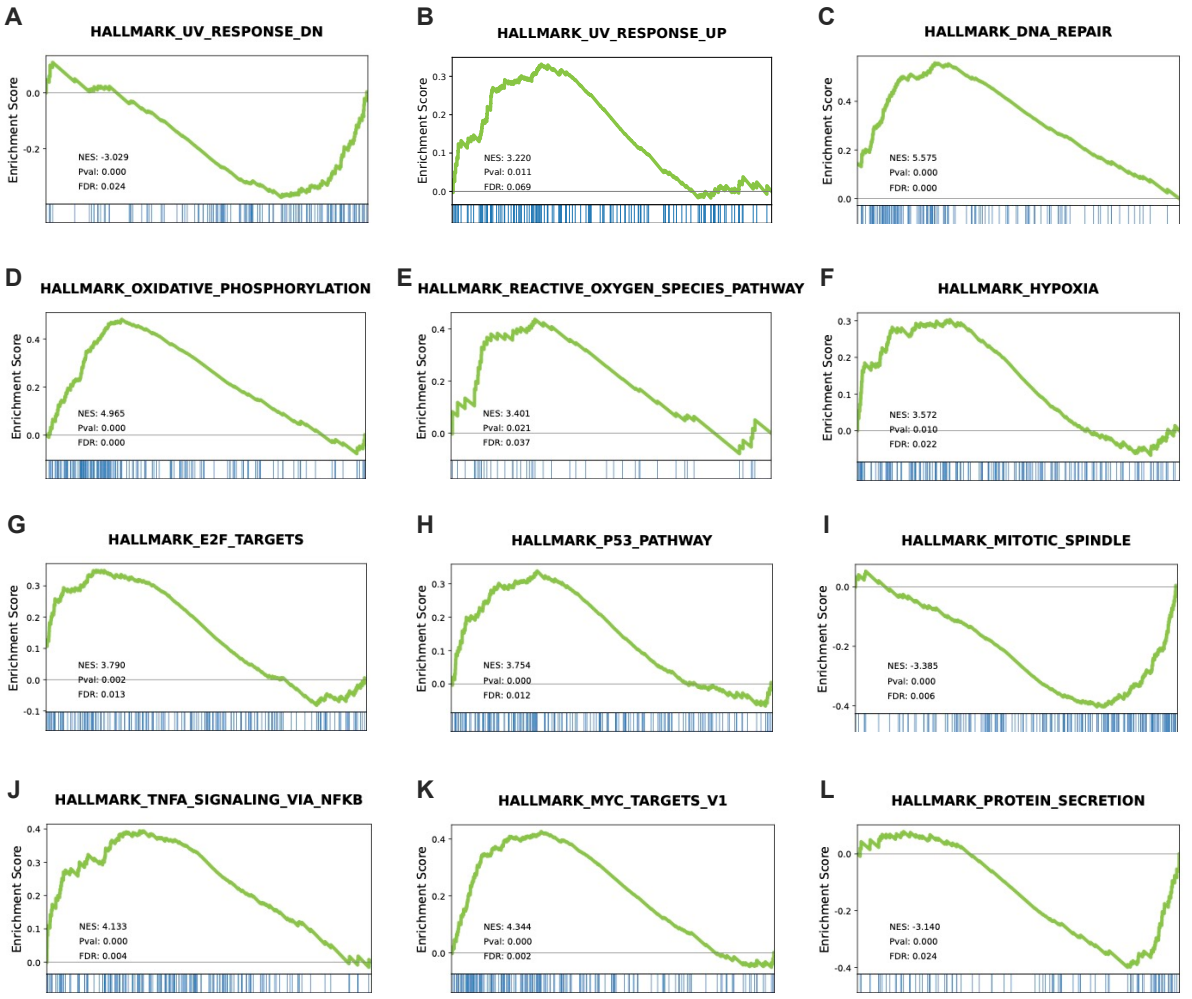

Figure 17. Enrichment plots representing significant up or down regulation of genes identified in pathways within the hallmarks of aging from C57BL/6 20-month-old female mouse hippocampal tissue. A. Enrichment plot displaying a downregulation of genes associated with the UV response pathway in female mice treated with GHK-Cu versus saline. B. Enrichment plot displaying an upregulation of genes associated with the UV response pathway in female mice treated with GHK-Cu versus saline. C. Enrichment plot displaying an upregulation of genes associated with the DNA repair pathway in female mice treated with GHK-Cu versus saline. D. Enrichment plot displaying an upregulation of genes associated with the oxidative phosphorylation pathway in female mice treated with GHK-Cu versus saline. E. Enrichment plot displaying an upregulation of genes associated with the reactive oxygen species pathway in female mice treated with GHK-Cu versus saline. F. Enrichment plot displaying an upregulation of genes associated with the hypoxia pathway in female mice treated with GHK-Cu versus saline. G. Enrichment plot displaying an upregulation of genes associated with the E2F target pathway in female mice treated with GHK-Cu versus saline. H. Enrichment plot displaying an upregulation of genes associated with the p53 pathway in female mice treated with GHK-Cu versus saline. I. Enrichment plot displaying a downregulation of genes associated with the mitotic spindle pathway in female mice treated with GHK-Cu versus saline. J. Enrichment plot displaying an upregulation of genes associated with the TNF-α signaling via NF-κB pathway in female mice treated with GHK-Cu versus saline. K. Enrichment plot displaying an upregulation of genes associated with the MYC (V1) target pathway in female mice treated with GHK-Cu versus saline. L. Enrichment plot displaying a downregulation of genes associated with the protein secretion pathway in female mice treated with GHK-Cu versus saline. $p<0.05$, FDR <0.1, n=3/cohort.

RNA-sequencing reveals mitotic spindle, UV response, and androgen-related brain aging pathways in male mice are improved with a five-day treatment of GHK-Cu.

In addition to the female cohort, hippocampal tissue from male mice treated with GHK-Cu and male mice receiving the saline control underwent RNA isolation, RNA sequencing, differential gene expression, and gene set enrichment analysis were completed to explore differences in gene expression and within the hallmark gene sets between the treated and control cohorts. Each enrichment plot displays the normalized enrichment score (NES) which assesses the significance and direction of gene expression, the p-value, and the false discovery rate (FDR). The enrichment score (ES) on the y-axis represents if the genes within the pathways of interest are upregulated, above the zero threshold, or downregulated, below the zero threshold. The number of pathways with significant up or downregulation in males is less than the females which presents another aspect of sex dependent phenotypes. The gene hallmark pathways for representing mitotic spindle function and downregulation of UV response are both downregulated in male mice treated with GHK-Cu compared to male mice receiving saline (Figure 17A & 17B). These pathways being downregulated follow the same trend seen in the females in Figure 16A and 16I. A pathway that was not affected in the females but was in the males is genes involved in the androgen response which is involved in sexual development in youth and cognitive function during the aging process. Male mice treated with GHK-Cu had increased downregulation of genes associated with the androgen response compared to the control cohort (Figure 17C). Though the male mice do not have as many pathways affected by GHK-Cu treatment as the female mice after statistical correction with FDR, the differences observed in Figure 17 are similar to what was observed in Figure 16 with the female cohorts.

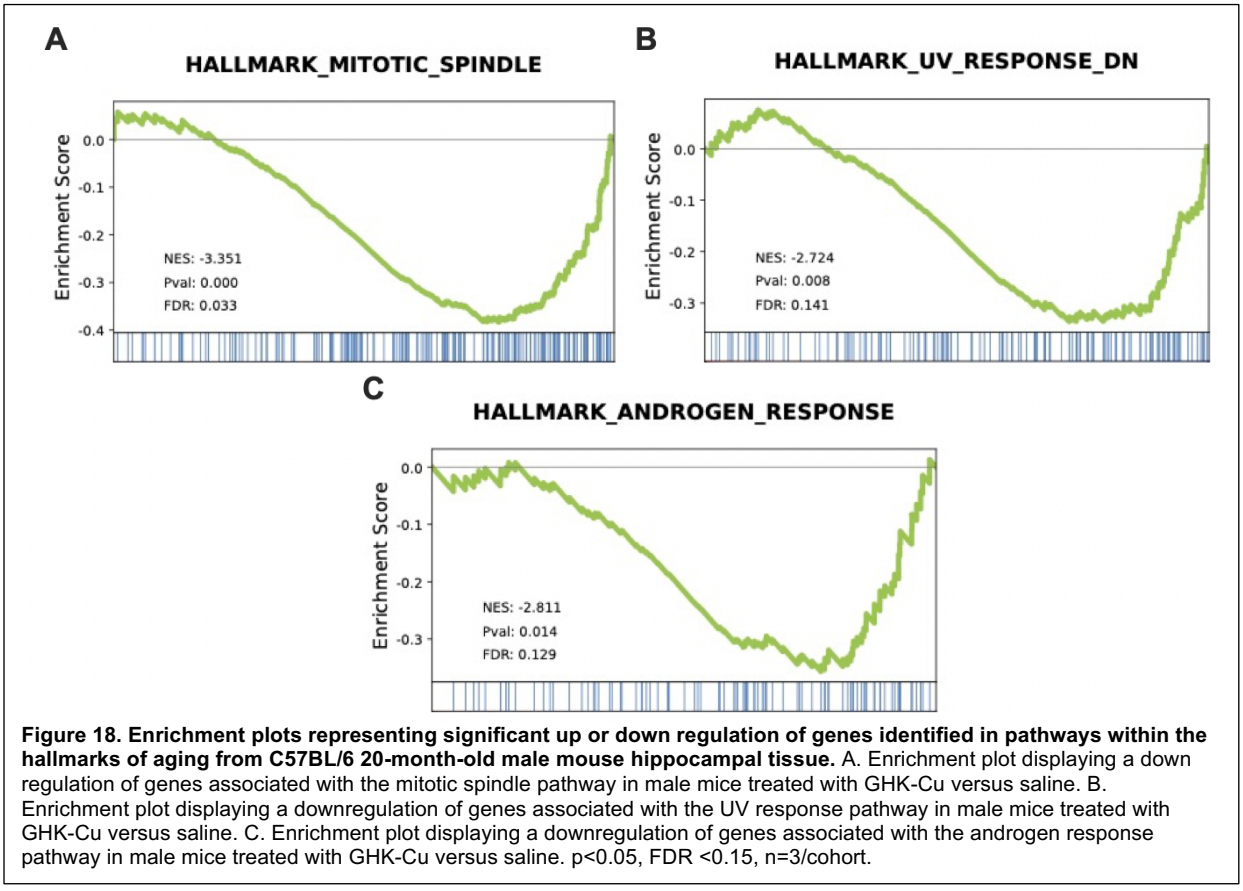

Figure 18. Enrichment plots representing significant up or down regulation of genes identified in pathways within the hallmarks of aging from C57BL/6 20-month-old male mouse hippocampal tissue. A. Enrichment plot displaying a down regulation of genes associated with the mitotic spindle pathway in male mice treated with GHK-Cu versus saline. B. Enrichment plot displaying a downregulation of genes associated with the UV response pathway in male mice treated with GHK-Cu versus saline. C. Enrichment plot displaying a downregulation of genes associated with the androgen response pathway in male mice treated with GHK-Cu versus saline. $p<0.05$, FDR <0.15, n=3/cohort.

RNA-sequencing reveals similarities across up and downregulation of gene pathways between male and female mice treated with GHK-Cu for five days.

Though there was a decreased amount of identified pathways with significant up or downregulation in males compared to females once statistically corrected with FDR, there were several non-significant pathways overlapping between the two sexes that had similar trends. Figure 18A and 18B reveal a non-significant trend of upregulation in males treated with GHK-Cu compared to the control cohort which aligns with the significant upregulation of both pathways in treated females as well (Figure 16C & 16D). This pattern is maintained with genes associated with the E2F and p53 pathways, both involved in cell cycle regulation. Male treated mice have a non-significant trend of upregulation compared to male mice receiving saline (Figure 18C & 18D). Once again, these same pathways are also upregulated in female mice receiving the treatment (Figure 16G &16H). Though some pathways were regulated in a sex-dependent manner including UV response of upregulated genes, ROS, hypoxia, TNF-α signaling via NF-κB, MYC V1 targets, and protein secretion, but some pathways are conserved across both sexes including the mitotic spindle pathway and UV response of downregulated genes.

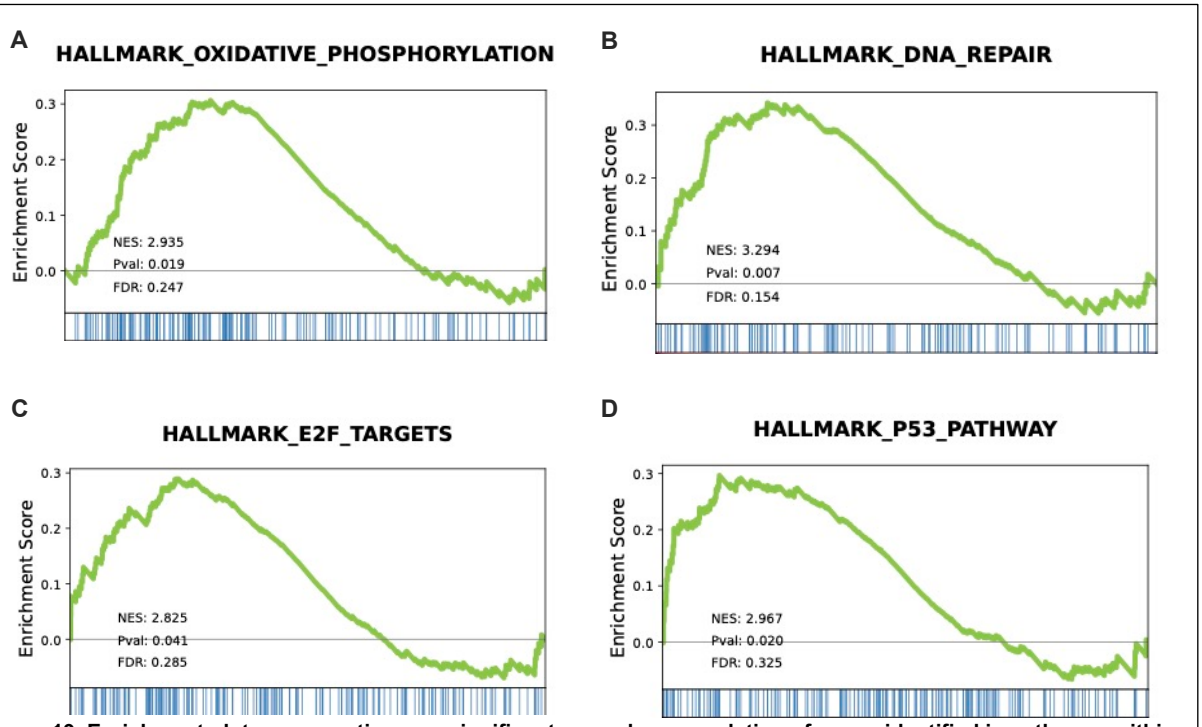

Figure 19. Enrichment plots representing non-significant up or down regulation of genes identified in pathways within the hallmarks of aging from C57BL/6 20-month-old male mouse hippocampal tissue. A. Enrichment plot displaying a non-significant upregulation of genes associated with the oxidative phosphorylation pathway in male mice treated with GHK-Cu versus saline. B. Enrichment plot displaying a non-significant upregulation of genes associated with the DNA repair pathway in male mice treated with GHK-Cu versus saline. C. Enrichment plot displaying a non-significant upregulation of genes associated with the E2F target pathway in male mice treated with GHK-Cu versus saline. D. Enrichment plot displaying a non-significant upregulation of genes associated with the p53 pathway in male mice treated with GHK-Cu versus saline. $p<0.05$, FDR >0.15, n=3/cohort.

Summary of RNA-sequencing highlights up and downregulation differences across sexes.

The Hallmark gene pathways that were identified through RNA sequencing reveal complex mechanisms and differences between sexes. The pathways identified for the female mice were numerous and spanned across several pathways such as cell cycle regulation, inflammation,

and oxidation. The pathways identified in the male mice were smaller in number compared to the females but maintained similar trends in up or downregulation. The table below summarizes the RNA sequencing findings based on the GSEA Hallmark gene pathways.

Females		Males	
GSEA Hallmark Pathway	**Regulation**	**GSEA Hallmark Pathway**	**Regulation**
UV Response DN	downregulation	Mitotic Spindle	downregulation
UV Response UP	upregulation	UV Response DN	downregulation
DNA Repair	upregulation	Androgen Response	downregulation
Oxidative Phosphorylation	upregulation		
Reactive Oxygen Species	upregulation		
Hypoxia	upregulation		
E2F Targets	upregulation		
p53	upregulation		
Mitotic Spindle	downregulation		
TNF-α signaling via NF-κB	upregulation		
MYC Targets V1	upregulation		
Protein Secretion	downregulation		

Table 1. A summary of the GSEA Hallmark gene pathways identified to be up or downregulated from C57BL/6 20-month-old female and male hippocampal tissue. The left side of the table displays the GSEA Hallmark gene pathways and regulation changes that were identified from RNA sequenced from the C57BL/6 female mouse hippocampus tissues. The right side of table displayed the GSEA Hallmark gene pathways and regulation changes that were identified from RNA sequenced from the C57BL/6 male mouse hippocampus tissues. n=3/cohort.

Discussion

Multiple methodologies were used to assess the effect on cognitive function of a five-day treatment of GHK-Cu on 20 -month-old C57BL/6 mice via intraperitoneal injection including a behavioral assay, immunohistochemistry staining of the brain, and RNA sequencing of hippocampal tissue. The behavioral assay, the Box Maze, revealed quicker escape times and increased memory and learning capability in male mice treated with GHK-Cu when compared to the control cohort, but introduced sex-dependency as the same trend was not observed in female mice. IHC revealed evidence of rescued cognitive function in treated mice with decrease in p21, MCP-1, TGF-β, and GFAP. These IHC results align with the hypothesized effect of GHK-Cu as it is known to be involved in the TGF-β/SMAD pathway that regulates several age-related processes including astrocytes. The RNA sequencing results add further robust evidence as to GHK-Cu's mechanisms and what pathways are impacted with a short-term treatment. RNA sequencing continued to reveal sex-dependent phenotypes with female mice experiencing more significant differences between treatment and control groups than male mice did, however trends between pathways remained consistent. Several pathways involved in key aging mechanisms such as DNA repair and oxidative phosphorylation were observed to increase in treated females when compared to females who received saline, further supporting GHK-Cu as a gerotherapeutic.

Cognitive Impairment. Cognitive function was assessed by a spatial navigation learning task, the Box Maze, validated to assess for cognitive impairment in aging mice (Darvas, 2020). In

aging C57BL/6 mice specifically, several assays including the Morris Water Maze and Novel Object Recognition have shown age-related cognitive decline developing as early as six months (Hendrickx et al., 2022). Within this mouse model, cognitive function continues to decline with 20-28-month-old mice undergoing the radial water tread maze experiencing increased cognitive decline with longer escape times compared to younger mice (Pettan-Brewer et al., 2013). 20-month-old C57BL/6 mice were identified as a model for resilience through evaluation of variation within their cohort, separation into ARCD susceptible and ARCD resistant cohorts, and significant differences in neuroinflammation (Daneshjoo et al., 2022). The variation and separation into susceptible and resistant cohorts mirrors natural variation in human aging with some cases maintaining cognitive function but having severe AD pathology on post-mortem examination (de Vries et al., 2024). The Learning Index values displayed in Figure 5 consider this variance on a population-wide level as an alternative way to assess Box Maze outputs. Figure 5 also introduces the first of many results that are different in a sex-dependent manner with Figure 5A displaying a significant difference between the male cohorts, but Figure 5B displays similar Learning Index values for both female cohorts. Further investigation into the C57BL/6 mouse model validated cognitive differences 12 and 20-month-old mice in novel location and spatial water maze performance, as well as presented several sex differences with 20-month-old females experiencing a decrease in spatial bias when compared to young and middle-aged female mice, and decreased spatial memory capability compared to males of the same age group in Y Maze (Benice et al., 2006 & Tucker et al., 2016). One possibility for the sex-dependent phenotype is a more severe level of cognitive impairment in the females that could not be reversed enough to reflect improvement in a behavioral assay within the five-day treatment timeline. The raw escape time values follow this trend as well with several significant differences observed in the male treated cohort compared to the male control cohort (Figure 6A), however there is only one significant difference observed in the females which is between two trials of the control cohorts (Figure 6B). The trends seen in Figure 6A support the argument that a five-day treatment of GHK-Cu helps alleviate brain aging. This can be seen with the males treated with GHK-Cu having a significantly quicker escape time in Trial 2 when compared to the control cohort, and in the significant improvement in escape time between Trial 1 and Trial 2, and Trial 1 and Trial 3 within the GHK-Cu treated males. This displays improvement across Trials 2 and 3 when compared to Trial 1 for the treatment cohort and reflects a significant difference in learning and memory capability of male mice who received GHK-Cu compared to those who received the saline control. Due to the time constraints of the experimental timeline, additional behavioral assays were not able to be performed, however other assays such as Y Maze and Radial Water Tread Maze should be kept in mind for alternative assays to assess learning, memory, and cognitive function (Kraeuter et al., 2019 & Pettan-Brewer et al., 2013).

Other aspects of the Box Maze reveal additional trends in exploratory behavior, learning, and sex-dependent phenotypes. Another parameter within the Box Maze for assessing memory is the number of false exit attempts a mouse makes into holes that are not the escape hole, with less false exits indicating better memory compared to more false exit attempts (Gawal et al., 2018). When compared between treated and control cohorts within each sex, not many notable significant differences were observed (Figure 8A & 8B). When comparing the average across all trials between males and females, it is observed that males treated with GHK-Cu have significantly less false exits compared to females treated with GHK-Cu (Figure 8C). This observation could be related to studies that have shown female C57BL/6 mice experienced decreased spatial bias and spatial memory capability compared to males as noted above (Benice et al., 2006 & Tucker et al., 2016).

Rearing can be an indicator of anxiety or exploratory behavior and is context-dependent with Sturman et al., 2018 differentiating supportive rearing, where the mouse rears up against a wall

or object, as an indication of exploratory behavior. As the majority of rearing performed in the Box Maze was supportive, it is within reason to interpret the trends as exploratory behavior in this context. Figure 7 reveals males treated with GHK-Cu for five days experiencing increased rearing in Trial 2 (Figure 7A), as well as females treated with GHK-Cu experiencing increased rearing in Trial 1, Trial 2, and when averaged across all trials (Figure 7B & 7C). Studies have shown similar levels of rearing across sex in younger C57BL/6 mice which is observed in the non-significant difference of the control cohorts in Figure 7C depicting the overall rearing average and further supports the argument that GHK-Cu is impacting exploratory behavior, more so in females than males (Reiber et al., 2022). To further evaluate this, future studies evaluating effects of GHK-Cu may incorporate an Open Field Test to specifically target the assessment of anxiety and exploratory behaviors (Seibenhener & Wooten, 2015).

TGF- β and Astrocyte Pathway. TGF-β, a transforming growth factor that helps regulate cell growth and differentiation, is involved in many age-related pathways and can be influenced by GHK-Cu. TGF-β levels have been shown to increase with age, as well as elevate in response to brain injury specifically in microglia and astrocytes (Finch et al., 1993 & Doyle et al., 2010). TGF-β levels in humans were found to be elevated in patients with ARCD when compared to the control cohort, and even higher in patients with Alzheimer's Disease when compared to those with ARCD (Park et al., 2021). This connects elevated levels of TGF-β with neurodegenerative diseases and a decline in cognitive function. Additionally, TGF-β has been identified to be a key regulator of astrocytes via the SMAD pathway with TGF-β requiring activation in the extracellular matrix, binding to receptors which phosphorylate SMAD2 and SMAD3, form a complex with SMAD4, bind to the SMAD binding element (SBE), and regulate expression of TGF-β-related genes (Luo et al., 2022). This has been connected to several astrocyte-related pathways including neurons secreting TGF-β to induce GFAP expression, neurogenesis, and inflammatory responses that are context-dependent (Sousa et al., 2004, Reilly et al., 1998, de Sampaio et al., 2002, & Buckwalter et al., 2006).

Immunohistochemistry was used to assess multiple aspects of this TGF-β/SMAD pathway. Figure 9 displays significantly decreased expression of TGF-β in both the hippocampus and cerebellum of male mice treated with GHK-Cu compared to male mice who received the control (Figure 9A, 9C, 9D, & 9F). Another sex-dependent phenotype was observed with no significant difference in TGF-β expression observed between the female cohorts (Figure 9A, 9C, 9D, & 9F). The same pattern was seen when staining for GFAP, a marker of astrocytes, which revealed decreased expression of GFAP in males in both the hippocampus and cerebellum, but not in females (Figure 10A, 10C, 10D, & 10F). It has been shown *in vivo* and *in vitro* that GHK-Cu inhibits TGF-β, which was further confirmed in a study evaluating GHK-Cu for a potential treatment of pulmonary fibrosis and revealed a decrease in TGF-β, phosphorylated SMAD2, phosphorylated-SMAD3, and inflammation with GHK-Cu treatment (Zhou et al., 2017). The results in Figure 9 and Figure 10 align with what was hypothesized with a decrease in TGF-β and GFAP with GHK-Cu treatment, however Figure 12 reveals unexpected results within this pathway. IHC of phosphorylated-SMAD2 reveals no significant change in stain percentage and expression of phosphorylated-SMAD2 within either sex, treatment and control cohorts, or brain region (Figure 12). This may indicate a disruption to the suspected TGF-β/SMAD pathway in relation to the phosphorylation of SMAD2, but no overall cascade disruption as the GFAP decrease is still observed as expected. Potential ways to evaluate this could be to assess multiple aspects of the TGF-β/SMAD pathway in response to GHK-Cu treatment such as levels of SMAD2, phosphorylated-SMAD3, the complex formed with SMAD4, and SBE binding levels.

An additional nuance to consider with the effects of GHK-Cu on TGF-β are the downstream impacts this decrease of TGF-β and GFAP has on astrocyte-related pathways. Astrocytes are

an important cell in the central nervous system and have a variety of functions such as promoting synapse formation and health of neurons. However, the level of astrocytes, and their biomarker GFAP, are known to increase in response to brain injury and can produce a reactive phenotype associated with inflammation and dysfunction of neuronal maintenance (Amalia, 2021). Elevated levels of astrocytes, astrocyte dysfunction, and senescent astrocytes have been linked to ARCD and several other neurodegenerative diseases with an increase in GFAP in areas surrounding Alzheimer's disease pathology such as Aβ plaques and tau (Csipo et al., 2019 & Kim et al., 2023). Pro-inflammatory cytokine signaling, often seen increased with an increase in GFAP, was observed in a mouse model of multiple sclerosis and was accompanied with memory deficits, further connecting astrocytes with cognitive function and ARCD (Osso & Chan, 2015). As discussed, there was a decrease in the expression of GFAP in IHC staining of the hippocampus and cerebellum in male mice treated with GHK-Cu for five-days compared to male mice who received saline (Figure 11A, 11C, 11D, & 11F). Synaptophysin, a marker of pre-synaptic health, and PSD95, a marker of post-synaptic health, were evaluated via IHC of the hippocampus and cerebellum, but revealed no significant differences across treatment cohorts, sex, or brain region (Figure 13 & Figure 14). This could indicate several things, one of which being that there is a decrease in the reactive and/or senescent forms of astrocytes due to the GHK-Cu treatment, but synaptic health and function remain unchanged from the control cohorts. To explore further, additional assays could be done to differentiate between different astrocyte types as GFAP is unable to do so. Additional markers could include complement component 3 (C3) which was observed to be secreted by astrocytes in response to brain injury and neurodegenerative disease development, S100A10 which is observed in reactive astrocytes that are activated in response to brain inflammation, or Lcn2 and Serpina3n, both found to be markers of reactive astrocytes via profile gene expression of various reactive astrocyte populations (Yang et al., 2024, Zhao et al., 2023, & Zamanian et al., 2012).

The IHC results revealing a decrease in TGF-β and GFAP in males treated with GHK-Cu aligns well with other assays explored in this experiment. Figure 5 and Figure 6 displaying the Learning Index scores and Box Maze escape times respectfully align with these results as well with the male mice treated with GHK-Cu experiencing a significantly improved Learning Index score and quicker escape times when compared to the cohort that received saline. These findings, along with other studies such as Park et al., 2021 that have found potential correlations between increased TGF-β levels and ARCD provide further data that supports the connection between TGF-β and cognitive function. Additionally, the RNA sequencing data in the hippocampus of male mice provide additional support for this connection. Male mice treated with GHK-Cu were found to have downregulation of the mitotic spindle pathway (Figure 18A) which can be an indicator of cancer in some contexts, but beneficial in others (Kienitz et al., 2005). However in this context, there is a clear link between TGF-β levels, mitotic spindle function, and the spindle checkpoint system via Survivin, an inhibitor of apoptosis (Lee et al., 2013). The relationship between TGF-β levels and androgen response is also complex and of interest as male mice treated with GHK-Cu experienced a downregulation of genes associated with the androgen response pathway (Figure 18C). Androgen deprivation therapy, targeted for prostate cancer treatment, has been noted to have potential negative impacts on cognitive function, however the majority of studies evaluated in a review on this topic found no significant change (Shim et al., 2022 & Andela et al., 2021). More exploration into this pathway is needed to definitively claim whether this is a negative or positive effect on cognitive function in aging animal models.

Cellular Senescence and MYC Pathway. Cellular senescence occurs when a cell enters an irreversible replicative arrest but is resistant to apoptosis and known to increase with age and age-related diseases (Wissler Gerdes et al., 2020). p21, a cyclin-dependent kinase also referred

to as CDKn1a, has many roles ranging from cell cycle inhibition to inducing apoptosis, but is known to induce cellular senescence via the p53/p21 pathway (Yan et al., 2024 & Khosla et al., 2020). In evaluating p21 expression via immunohistochemistry, it was observed that females treated with GHK-Cu for five-days experienced decreased p21 expression due to having less percent area of positive staining in both the hippocampus and cerebellum (Figure 15A & 15D). Males treated with GHK-Cu were also observed to have a decrease in p21 expression, but only in the cerebellum (Figure 15D). This aligns well when compared to the RNA-sequencing results of the hippocampal tissue of these mice which revealed an upregulation in the p53 and MYC pathways in females treated with GHK-Cu, but not a significant upregulation in the treated male cohort (Figure 17H & 16K, Figure 19). Typically, an upregulation of p53 and MYC pathways are related to a repression of p21 (Gartel & Radhakrishnan, 2005). In studies focused on the overexpression of c-MYC, it was found that the overexpression of MYC, increase of p53, and decrease of p21 led to a shift from cell cycle arrest to inducing apoptosis which was noted to be beneficial in potential cancer therapies (Seoane et al., 2002). The shift from cell cycle arrest to apoptosis is extremely advantageous in ARCD as cell cycle arrest can lead to senescent cells which accumulates dysfunctional cells, whereas an increase of apoptosis can increase the removal of damaged cells (Arguelles et al., 2019). This suspected mechanism aligns with the observed results in both IHC and RNA sequencing and implies positive effects as a result of GHK-Cu treatment. A potential explanation for the sex-dependent phenotype is that female C57BL/6 mice 22-25-months old have been shown to have higher cellular senescent expression in the hippocampus compared to male mice, specifically in microglia which is also known to express p21 when senescent (Ocanas et al., 2023 & Mastudaira et al., 2023). Additional antibodies of interest for future IHC to strengthen this argument includes IBA-1, a marker of microglia, and BCL2L, a marker of microglia associated with senescence and inflammation (Drake et al., 2024).

This suspected pathway is complex and has other mechanisms involved, one of which being E2F, a transcription factor involved in cell cycle regulation and DNA synthesis. GSEA was performed on wound tissue form young and aged C57BL/6 mice which revealed a downregulation in the E2F pathway in aged macrophages when compared to the younger cohort (Dube et al., 2022). This indicates an age-related change in the E2F pathway that contributes to decreased DNA repair and altered cell cycle progression, but was a target affected by the five-day treatment of GHK-Cu. Figure 16G shows the upregulation of E2F in the hippocampal tissue of females treated with GHK-Cu. E2F is a known regulator of cellular apoptosis via both p53-dependent and independent pathways (Stanelle et al., 2002). The upregulation of E2F has also been shown to result in activation of other transcription factors such as MYC and further contributes to the involvement and suspected pathway of E2F, p53, and MYC being involved in decreased cellular senescence and increased apoptosis (Stanelle et al., 2002).

Oxidative phosphorylation is an extremely important energy-producing mechanism tied to oxygen supplies to the brain and cognitive function. Impaired oxidative phosphorylation function and oxidative stress can lead to brain aging, ARCD, and numerous neurodegenerative diseases (Singh et al., 2022). It was also found that MYC can impact oxidative phosphorylation, with several studies showing expression of MYC can result in positive regulation of oxidative phosphorylation and glycolysis (Goetzman & Prochownik, 2018). Female mice treated with GHK-Cu experienced a significant upregulation of the oxidative phosphorylation pathway compared to female mice who received the saline control (Figure 17D). This aligns with the upregulation of the MYC pathway observed in female treated mice as well, further connecting these mechanisms (Figure 17K). Though MYC impacts oxidative phosphorylation in a seemingly positive context, there are other RNA sequencing pathways potentially impacted by

MYC that are complex and could lead to negative effects including reactive oxygen species (ROS) and hypoxia. ROS, a sign of oxidative stress and dysfunction, is often upregulated in later age and in tandem with neurodegenerative diseases (Kim et al., 2024). It can disrupt cellular processes, synaptic transmission, and worsen chronic inflammation which are all associated with brain aging, so much so that ROS is targeted when investigating gerotherapeutics (Kim et al., 2024). Hypoxia, a state of reduced oxygenation, can lead to several similar processes including cellular senescence and the development of neurodegeneration, and is closely tied to age-related diseases (Nisar et al., 2024). Unexpectedly, RNA sequencing of the hippocampal tissue of female mice treated with GHK-Cu for five days revealed upregulation of ROS and hypoxia compared to the control cohort (Figure 17E & 17F). There is an established link between MYC and hypoxia via hypoxia-inducible factors (HIFs) in a cancerous context to promote the growth of cancer cells, but this could provide an explanation as to why the hypoxia pathway is upregulated in female mice treated with GHK-Cu versus female mice who received saline (Li et al., 2020). This trend was not observed in the male mice with a non-significant upregulation of the oxidative phosphorylation pathway and no notable regulation differences of the ROS or hypoxia pathways (Figure 19A). This difference could highlight a reason why the female mice treated with GHK-Cu did not show significantly different cognitive function compared to their control cohort in the Box Maze assay when analyzing Learning Index scores or escape time (Figure 5 & Figure 6). Further investigation into this pathway is warranted as the upregulation of ROS and hypoxia can have negative impacts to cognitive function and neurodegenerative diseases, and could point to a sex-dependent phenotype.

Inflammation. Chronic inflammation is a key hallmark of aging and has been linked to worsening cognitive function, development of dementia, neurodegeneration, and other chronic illnesses (Sartori et al., 2013). MCP-1, a monocyte chemoattractant protein responsible for recruiting monocytes, is a marker for inflammation and a potential biomarker of aging as levels have been observed to increase in both mice and humans with increasing age and frailty (Yousefzadeh et al., 2017). A significant decrease of MCP-1 expression and intensity is observed in both the hippocampus and cerebellum of male mice treated with GHK-Cu in a sex-dependent manner (Figure 16A, 16C, 16D, & 16F). Monocyte recruitment and the role of MCP-1 was shown to be increased in male mice compared to female mice which presents a sex-dependent phenotype related to MCP-1 prior to treatment (Varghese et al., 2022). Additionally, an eight-week treatment of GHK-Cu in C57BL/6 mice revealed a significant decrease in MCP-1 expression in female treated mice, as well as a nonsignificant trend of decreasing MCP-1 expression in male mice (Tucker et al., 2023). Both sexes of mice treated for eight weeks also experienced quicker escape times from the spatial navigation learning task, whereas only the treated male cohort treated for five days had quicker escape times compared to the control cohort (Figure 6A) (Tucker et al., 2023). This supports the connection between MCP-1 and cognitive decline, as well as a longer treatment of GHK-Cu being successful in alleviating cognitive decline observed in females.

Another inflammatory pathway of interest is TNF-α signaling via NF-κB which is an inflammatory signaling pathway known to increase with age and result in cellular senescence, apoptosis, and inflammatory responses (Garcia-Garcia et al., 2021). The gene set involved in TNF-α signaling via NF-κB was observed to be upregulated in female mice treated with GHK-Cu compared to the control cohort in hippocampal tissue (Figure 17J). This was unexpected as several publications reported GHK-Cu resulting in a decrease in inflammation and TNF-α signaling, however many of those publications are treating very C57BL/6 mice of 8-10 weeks (Ma et al., 2020, Zhang et al., 2022, & Park JR et al., 2016). One explanation for the upregulation seen in

this experiment may be the connection to the MYC pathway, and the relationship between MYC expression and increased sensitivity of negative effects caused by TNF-α (Klefstrom et al., 1994). It is also important to note the relationship between TNF-α and MCP-1, with TNF-α typically upregulating the expression of MCP-1 (Yang et al., 2009). This was not observed in the IHC data with MCP-1 expression and staining intensity in the hippocampus and cerebellum remaining non-significant between the female mice who received GHK-Cu versus saline (Figure 16). Much like ROS and hypoxia, this upregulation was not observed in males treated with GHK-Cu and could be an indication of what mechanisms are contributing to the observed sex-dependent phenotypes in the Box Maze assay, IHC, and RNA sequencing differences.

Summary & Conclusion

In conclusion, a five-day treatment of GHK-Cu resulted in increased resilience to brain aging and rescued age-related cognitive decline in middle-aged male mice not female mice. Male mice treated with GHK-Cu experienced greater capacity for learning, memory, and cognitive function shown by the Box Maze assay and IHC staining of several key markers involved in brain aging and GHK-Cu pathways including decreased TGF-β, GFAP, p21, and MCP-1 staining expression and intensity. This study revealed several sex-dependent phenotypes with treated male mice experiencing increased cognitive function and decreased inflammation, however across several assays with female treated mice not experiencing a significant difference from female mice receiving saline in Learning Index or escape times associated with the Box Maze. Additionally, IHC staining revealed several different trends in the female cohorts when compared to the male cohorts with treated females seeing decreased cellular senescence and treated males experiencing decreased inflammation and the expected inhibition of the TGF-β pathway. RNA sequencing added data that showed pathways being upregulated such as oxidative phosphorylation and DNA repair, as well as some potential negative pathways being upregulated including TNF-α signaling via NF-κB and reactive oxygen species specifically in female mice. These observations provide useful information for further studies focused on GHK-Cu treatment of age-related diseases and potential explanations for the sex-dependent differences.

References

Almeida J, Martins AR, Amaral L, *et al.* The cerebellum is causally involved in episodic memory under aging. *GeroScience,* 2023, 45: 2276-2287. [Crossref]

Amalia L. Glial Fibrillary Acidic Protein (GFAP): Neuroinflammation Biomarker in Acute Ischemic Stroke. *J Inflamm Res,* 2021 14: 7501-7506. [Crossref]

Andela CD, Matte R, Jazet IM, *et al.* Effect of androgen deprivation therapy on cognitive functioning in men with prostate cancer: A systematic review. *Int J Urol,* 2021, 28(8): 786-798. [Crossref]

Arguelles S, Guerrero-Castillo A, Cano M, *et al*. Advantages and disadvantages of apoptosis in the aging process. *NY Academy of Science,* 2019, 1443(1): 20-33. [Crossref]

Benice TS, Rizk A, Kohama S, *et al.* Sex-differences in age-related cognitive decline in C57BL/6J mice associated with increased brain microtubule-associated protein 2 and synaptophysin immunoreactivity. *Neuroscience,* 2006, 137(2): 413-423. [Crossref]

Bettio LEB, Rajendran L, & Gil-Mohapel J. The effects of aging in the hippocampus and cognitive decline. *Neuroscience & Biobehavioral Reviews,* 2017, 79: 66-86. [Crossref]

Buckwalter MS, Yamane M, Coleman BS, *et al.* Chronically increased transforming growth factor-beta1 strongly inhibits hippocampal neurogenesis in aged mice. *Am J Pathol,* 2006, 169(1): 154-164. [Crossref]

Cohen J & Torres C. Astrocyte senescence: Evidence and significance. *Wiley Aging Cell,* 2019, [Crossref]

Csipo T, Lipecz A, Ashpole NM, *et al.* Astrocyte senescence contributes to cognitive decline. *GeroScience,* 2019, 42(1): 51-55. [Crossref]

Daneshjoo S, Park JY, Moreno J, *et al.* A mouse model of naturally occurring age-related cognitive impairment. *Aging Pathobiology and Therapeutics,* 2022, 4(3): 87-89. [Crossref]

Darvas M, Mukherjee K, Lee A, & Ladiges W. A Novel One-Day Learning Procedure for Mice. *Current Protocols,* 2020. [Crossref]

de Sampaio TCL, Martinez R, da Silva EF, *et al*. Neuro-glia interaction effects on GFAP gene: a novel role for transofring growth factor-β1. *European Journal of Neuroscience,* 2002, 16(11): 2059-2069. [Crossref]

de Vries LE, Huitinga I, Kessels HW, *et al.* The concept of resilience to Alzheimer's Disease: current definitions and cellular and molecular mechanisms. *BMC Mol Neurodegeneration,* 2024, 19(33). [Crossref]

Doyle KP, Cekanaviciute E, Mamer LE, *et al.* TGFβ signaling in the brain increases with aging and signals to astrocytes and innate immune cells in the weeks after stroke. *J of Neuroinflammation*, 2010, 62. [Crossref]

Drake SS, Zaman A, Gianfelice C, *et al.* Senolytic treatment diminishes microglia and decreases severity of experimental autoimmune encephalomyelitis. *J of Neuroinflammation,* 2024. [Crossref]

Dube CT, Ong YHB, Wemyss K, *et al.* Age-Related Alterations in Macrophage Distribution and Function Are Associated With Delayed Cutaneous Wound Healing. *Front. Immun,* 2022. 13. [Crossref]

Eshkoor SA, Hamid TA, Mun CY, & Ng CK. Mild cognitive impairment and its management in older people. *Clin Interv Aging,* 2015, 10(10): 689-693. [Crossref]

Finch CE, Laping NJ, Morgan TE, *et al*. TGF-beta1 is an organizer of responses to neurodegeneration. *J Cell Biochem*, 1993, 53(4): 314-322. [Crossref]

Garcia-Garcia VA, Alameda JP, Page A, *et al.* Role of NF-κB in Ageing and Age-Related Diseases: Lessons from Genetically Modified Mouse Models. *Cells,* 2021, 10(8). [Crossref]

Gartel AL & Radhakrishnan SK. Lost in Transcription: p21 Repression, Mechanism, and Consequences. *Cancer Research*, 2005, 65(10): 3980-3985. [Crossref]

Gawal K, Gibula E, Marszalek-Grabska M, *et al.* Assessment of spatial learning and memory in the Barnes maze task in rodents – methodological considerations. *NM's Archives of Pharmacology,* 2018, 392: 1-18. [Crossref]

Goetzman ES & Prochownik EV. The Role of MYC in Coordinating Glycolysis, Oxidative Phosphorylation, Glutaminolysis, and Fatty Acid Metabolism in Normal and Neoplastic Tissues. *Front. Endocrinol.,* 2018, 9. [Crossref]

Hale JM, Schneider DC, Mehta NK, & Myrskyla M. Cognitive impairment in the U.S.: Lifetime risk, age at onset, and years impaired. *SSM Popul Health,* 2020, 31(11): 100577. [Crossref]

He Q, Mazzola J, & Ladiges W. The naturally occurring peptide GHK reverses age-related fibrosis by modulating myofibroblast function. *Aging Pathobiology and Therapeutics,* 2024, [Crossref].

Hecker L, Logsdon NJ, Kurundkar D, Kurundkar A, Bernard K, Hock T, *et al*. Reversal of persistent fibrosis in aging by targeting Nox4-Nrf2 redox imbalance. *Sci Transl Med*, 2014, 6(231): 231ra247. [Crossref]

Hendrickx JO, De Moudt S, Calus E, *et al.,* Age-related cognitive decline in spatial learning and memory of C7BL/6J mice. *Behavioral Brain Research*, 2022, 418. [Crossref]

Hugo J & Ganguli M. Dementia and cognitive impairment: epidemiology, diagnosis, and treatment. *Clin Geriatr Med,* 2014, 30(3): 412-442. [Crossref]

Jognsiriyanyong S & Limpawattana P. Mild Cognitive Impairment in Clinical Practice: A Review Article. *Am J Alzheimers Dis Other Demen,* 2018, 33(8): 500-507. [Crossref]

Khosla S, Farr JN, Tchkonia T, *et al.* The role of cellular senescence in ageing and endocrine disease. *Naure Reviews Endocrinology,* 2020, 16: 263-275. [Crossref]

Kienitz A, Vogel C, Morales I, *et al.* Partial downregulation of *MAD1* causes spindle checkpoint inactivation and aneuploidy, but does not confer resistance towards taxol. *Nature Oncogene,* 2005, 24: 4301-4310. [Crossref]

Kim KY, Shin KY, & Chang KA. GFAP as a Potential Biomarker for Alzheimer's Disease: A Systematic Review and Meta Analysis. *Cells,* 2023, 12(9): 1309. [Crossref]

Kim S, Jung UJ, & Kim SR. Role of Oxidative Stress in Blood-Brain Barrier Disruption and Neurodegenerative Diseases. *Antioxidants*, 2024, 13(12): 1462. [Crossref]

Kirkland JL, Stout MB, & Sierra F. Resilience in Aging Mice. *The Journals of Gerontology,* 2016, 71(11): 1407-1414. [Crossref]

Kivipelto M, Mangialasche F, & Ngandu T. Lifestyle interventions to prevent cognitive impairment, dementia and Alzheimer disease. *Nat Revl Neurol*, 2018, 14(11): 653-666. [Crossref]

Klefstrom J, Vastrik I, Valle J, *et al.* c-Myc induces cellular susceptibility to the cytotoxic action of TNF-alpha. *EMBO J,* 1994, 13(22): 5442-5450. [Crossref]

Kraeuter AK, Guest PC & Sarnyai Z. The Y-Maze for Assessment of Spatial Working and Reference Memory in Mice. *Pre-Clinical Models*, 2019, 105-111. [Crossref]

Langa KM & Levine DA. The diagnosis and management of mild cognitive impairment: a clinical review. *JAMA,* 2014, 312(23): 2551-2561 [Crossref]

Lee J, Choi JH, & Joo CK. TGF-β1 regulates cell fate during epithelial-mesenchymal transition by upregulating survivin. *Cell Death & Disease,* 2013, 4(714). [Crossref]

Li Y, Sun XX, Qian DZ, & Dai MS. Molecular Crosstalk Between MYC and HIF in Cancer. *Front. Cell Dev. Biol.,* 2020, 8. [Crossref]

Liu H, Guo H, Jian Z, *et al*. Copper Induces Oxidative Stress and Apoptosis in the Mouse Liver. *Oxid Med Cell Longev,* 2020. [Crossref]

López-Otín C, Blasco MA, Partridge L, *et al.* Hallmarks of aging: An expanding universe. *Cell*, 2023, 186(2): 243-278. [Crossref]

Luo J. TGF-β as a Key Modulator of Astrocyte Reactivity: Disease Relevance and Therapeutic Implications. *biomedicines,* 2022. [Crossref]

Ma WH, Li M, Ma HF, *et al.* Protective effects of GHK-Cu in bleomycin-induced pulmonary fibrosis via anti-oxidative stress and anti-inflammation pathways. *Life Sciences,* 2020, 241. [Crossref]

Matias I, Morgado J & Gomes FCA. Astrocyte Heterogeneity: Impact to Brain Aging and Disease. *Frontiers in Aging Neuroscience,* 2019, 11(59). [Crossref]

Matsudaira T, Nakano S, Konishi Y, *et al.* Cellular senescence in white matter microglia is induced during ageing in mice and exacerbates the neuroinflammatory phenotype. *Communications Biology,* 2023. [Crossref]

Mayo Clinic. Mild cognitive impairment, 2024. [Crossref]

Murman DL. The Impact of Aging on Cognition. *Semin Hear*, 2015, 36(3): 111-121. [Crossref]

Nichols NR, Day JR, Laping NJ, *et al*. GFAP mRNA increases with age in rat and human brain. *Neurobiol. Aging,* 1993, 14(5): 421-429. [Crossref]

Nisar A, Khan S, Li W, *et al.* Hypoxia and aging: molecular mechanisms, diseases, and therapeutic targets. *MedComm*, 2024, 5(11): 786. [Crossref]

Ocanas SR, Pham KD, Cox JEJ, *et al*. Microglial senescence contributes to female-biased neuroinflammation in the aging mouse hippocampus: implications for Alzheimer's disease. *Journal of Neuroinflammation,* 2023, 188. [Crossref]

Osso LA & Chan JR. Astrocytes Underlie Neuroinflammatory Memory Impairment. *Cell,* 2015, 163(7): 1574-1576. [Crossref]

Park JK, Lee KJ, Kim JY, & Kim H. The Association of Blood-Based Inflammatory Factors IL-1β, TGF-β and CRP with Cognitive Function in Alzheimer's Disease and Mild Cognitive Impairment. *Psychiatry Investigation,* 2021, 18(1): 11-18. [Crossref]

Park JR, Lee H, Kim SI, & Yang SR. The tri-peptide GHK-Cu complex ameliorates lipopolysaccharide-induced cute lung injury in mice. *Oncotarget,* 2016, 7: 58405-58417. [Crossref]

Park JY & Ladiges W. A simple spatial navigation paradigm in aging mice connects heterogeneous behavioral phenotypes with neuropathology and Alzheimer's disease. *University of Washington Libraries,* 2024. [Crossref]

Pettan-Brewer C, Touch DV, Wiley JC, *et al.* A novel radial water tread maze tracks age-related cognitive decline in mice. *Pathobio of Aging,* 2013 3(1). [Crossref]

Pickart L, Freedman JH, Loker WJ, *et al.* Growth-modulating plasma tripeptide may function by facilitating copper uptake into cells. *Nature,* 1980, 288(5792): 715-7. [Crossref]

Pickart L & Margolina A. The Effect of the Human Plasma Molecule GHK-Cu on Stem Cell Actions and Expression of Relevant Genes. *OBM Geriatrics*, 2018, 2(3): 9. [Crossref]

Pickart L, Vasquez-Soltero JM, & Margolina A. GHK Peptide as a Natural Modulator of Multiple Cellular Pathways in Skin Regeneration. *BioMedResearch International,* 2015. [Crossref]

Pickart L, Vasquez-Soltero JM, & Margolina A. The Effect of Human Peptide GHK on Gene Expression Relevant to Nervous System Function and Cognitive Decline. *Brain Sci,* 2017, 7(2): 20. [Crossref]

Randhawa SS & Varghese D. Geriatric Evaluation and Treatment of Age-Related Cognitive Decline. *StatPearls,* 2023. [Crossref]

Reiber M, Koska I, Pace C, *et al.* Development of behavioral patterns in young C57BL/6J mice: a home cage-based study. *Scientific Reports,* 2022. [Crossref]

Reilly JF, Maher PA, & Kumari VG. Regulation of astrocyte GFAP expression by TGF-beta1 and FGF-2. *Glia,* 1998, 22(2): 202-210. [Crossref]

Sartori AC, Vance DE, Slater LZ, & Crowe M. The Impact of Inflammation on Cognitive Function in Older Adults Implications for Healthcare Practice and Research. *J of Neuroscience Nursing,* 2013, 44(4): 206-217. [Crossref]

Seibenhener ML & Wooten MC. Use of the Open Field Test to Measure Locomotor and Anxiety-like Behavior in Mice. *J Vis Exp.,* 2015, 96. [Crossref]

Seoane J, Le HV, & Massague J. Myc suppression of the p21(Cip1) Cdk inhibitor influences the outcome of the p53 response to DNA damage. *Nature,* 2002, 419 729-734. [Crossref]

Shim M, Bang WJ, Oh CY, *et al.* Androgen deprivation therapy and risk of cognitive dysfunction in men with prostate cancer: is there a possible link? *Prostate Int.,* 2022, 10(1): 68-74. [Crossref]

Singh P, Barman B, & Thakur MK. Oxidative stress-mediated memory impairment during aging and its therapeutic intervention by natural bioactive compounds. *Front. Aging Neurosci,* 2022, 14. [Crossref]

Sousa VDO, Romao L, Neto VM, & Gomes FCA. Glial fibrillary acidic protein gene promoter is differently modulated by transforming growth factor-beta 1 in astrocytes from distinct brain regions. *European Journal of Neuroscience,* 2004, 19(7): 1721-1730. [Crossref]

Stanelle J, Stiewe T, Theseling CC, *et al.* Gene expression changes in response to E2F1 activation. *Nucleic Acids Research,* 2002, 30(8): 1859-1867. [Crossref]

Sturman O, Germain PL, & Bohacek J. Exploratory rearing: a context- and stress-sensitive behavior recorded in the open-field test. *International Journal of the Biology of Stress,* 2018, 21(5): 443-452. [Crossref]

Tucker LB, Fu AH, & McCabe JT. Performance of Male and Female C57BL/6J Mice on Motor and Cognitive Tasks Commonly Used in Pre-Clinical Traumatic Brain Injury Research. *J Neurotrauma,* 2016, 33(9): 880-894. [Crossref]

Tucker, M, Keely A, Park JY, *et al.* Intranasal GHK peptide enhances resilience to cognitive decline in aging mice. *BioArchives,* 2023. [Crossref]

Varghese M, Clemente J, Lerner A, *et al.* Monocyte Trafficking and Polarization Contribute to Sex Differences in Meta-Inflammation. *Front. Endocrinol.,* 2022, 13. [Crossref]

Wilson RS, Leurgans SE, Boyle, PA, *et al.* Neurodegenerative basis of age-related cognitive decline. *Neurology,* 2010, 75(12): 1070-1078. [Crossref]

Wissler Gerdes EO, Zhu Y, Weigand BM, *et al.* Chapter Eight – Cellular senescence in aging and age-related diseases: Implications for neurodegenerative diseases. *International Review of Neurobiology,* 2020, 155: 203-234. [Crossref]

Yan J, Chen S, Yi Z, *et al.* The role of p21 in cellular senescence and aging-related diseases. *Molecules and Cells,* 2024, 47(11). [Crossref]

Yang J, Park Y, Zhang H, *et al.* Role of MCP-1 in tumor necrosis factor-a-induced endothelial dysfunction in type 2 diabetic mice. *Translational Physiology,* 2009, 297(4): H1208-H1216. [Crossref]

Yang K, Liu Y, & Zhang M. The Diverse Roles of Reactive Astrocytes in the Pathogenesis of Amyotrophic Lateral Sclerosis. *Brain Sciences,* 2024, 14(2): 158. [Crossref]

Yousefzadeh MJ, Schafer MJ, Hooten NN, *et al.* Circulating levels of monocyte chemoattractant protein-1 as a potential measure of biological age in mice and frailty in humans. *Aging Cell,* 2017, 17(2). [Crossref]

Zamanian JL, Xu L, Foo LC, *et al.* Genomic Analysis of Reactive Astrogliosis. *Journal of Neuroscience,* 2012, 32(18): 6391-6410. [Crossref]

Zhang Q, Yan L, Lu J, & Zhou X. Glycyl-L-histidyl-L-lysine-Cu(2+) attenuates cigarette smoke-induced pulmonary emphysema and inflammation by reducing oxidative stress pathway. *Front. Mol. Biosci.,* 2022, 9. [Crossref]

Zhau Q, Ren YL, Zhu YJ, *et al.* The origins and dynamic changes of C3- and S100A10-positive reactive astrocytes after spinal cord injury. *Cell Neuroscience,* 2023, 17. [Crossref]

Zhou XM, Wang GL, Wang XB, *et al.* GHK Peptide Inhibits Bleomycin-Induced Pulmonary Fibrosis in Mice by Suppressing TGFβ1/Smad-Mediated Epithelial-to-Mesenchymal Transition. *Front. Pharmacol.* 2017, Vol 8. [Crossref]